8-2012

Design and Synthesis of Boronic Acid-Based Sensors for Microarray Analysis and FRET-detection to study Carbohydrates

Yilin Wang
ywang63@utk.edu

To the Graduate Council:

I am submitting herewith a thesis written by Yilin Wang entitled "Design and Synthesis of Boronic Acid-Based Sensors for Microarray Analysis and FRET-detection to study Carbohydrates." I have examined the final electronic copy of this thesis for form and content and recommend that it be accepted in partial fulfillment of the requirements for the degree of Master of Science, with a major in Chemistry.

Michael D. Best, Major Professor

We have read this thesis and recommend its acceptance:

David C. Baker, Jon P. Camden

Accepted for the Council:
Carolyn R. Hodges

Vice Provost and Dean of the Graduate School

(Original signatures are on file with official student records.)

Design and Synthesis of Boronic Acid-Based Sensors for Microarray Analysis and FRET-Detection to Study Carbohydrates

A Thesis Presented for
The Master of Science Degree
University of Tennessee, Knoxville

Yilin Wang

August 2012

Acknowledgements

First and foremost, I offer my sincerest gratitude to my advisor, Dr. Michael Best, who has supported me throughout my thesis with his patience and knowledge. I attribute the level of my Masters degree to his encouragement and effort, and without him, this thesis would not have been completed. One simply could not wish for a more helpful advisor. When I run into difficulties, I can always count on him for kind words and helpful advice. I can say with absolute certainty that I would not be who I am today without his guidance.

I would also like to thank my committee members Dr. David Baker and Dr. Jon Camden for providing me with their time, knowledge, and insight while I worked on completing my thesis. In my daily work, I have been blessed with the friendly and cheerful Best group, past and present. I thank you for being my friends away from home. When I first started working in lab, Heidi Bostic and Chí-Linh Đo-Thanh trained me and taught me what I knew today. Without them, I would have been completely lost in lab.

Last but definitely not least, I would like to thank my parents for supporting me through all the obstacles I have encountered.

Abstract

Carbohydrates play significant roles in various biological and pathological processes such as cancer metastasis and inflammation. They participate in various signaling pathways and are able to bind to a litany of biological receptors such as proteins and viruses. Biologists have known for decades that the structures of glycans change with the onset of cancer and inflammation. Due to these important activities, carbohydrate sensing has long been a focus of research. One example of such a carbohydrate sensor is boronic acid-based sensors. Boronic acid-based sensors are of particular interest due to their selectivity for 1,2- or 1,3-diols. A variety of techniques have been employed for detection. Two techniques that have rarely been applied are high-throughput microarray analysis and FRET detection. In this thesis, we present work based on the development of a boronic acid-based carbohydrate sensor that will be used for microarray analysis and the development of various fluorophore-tagged boronic acids as donor/acceptor pairs for FRET detection. Herein, we describe the design and development of these compounds as well as initial results in their application for the detection of saccharides involved in important biological properties.

Table of Contents

List of Figures

Chapter 1: Design, Synthesis and Studies of Boronic Acid Based Carbohydrate Receptors

1.1 Background and Significance of Carbohydrates in Biological Processes

Carbohydrates, also known as saccharides, glycans or sugars, play numerous roles in living organisms. The carbohydrates are divided into four groups: monosaccharides, disaccharides, oligosaccharides, and polysaccharides. In general, monosaccharides and disaccharides are simple carbohydrates with low molecular weight, which are commonly referred to as sugars. Monosaccharides are the simplest and most basic units of carbohydrates; two units of monosaccharides condense to form a disaccharide. Even though the nature of carbohydrate nomenclature is complex, the names of these simple sugars very often end in the suffix –ose. For example, blood sugar is the monosaccharide glucose, table sugar is the disaccharide sucrose, and milk sugar is the disaccharide lactose. Oligosaccharides are polymers of sugars containing typically two to ten units of monosaccharides. In mammalian systems, they are generally found *O*- or *N*-linked to compatible amino acid side chains.[1] Polysaccharides are long carbohydrate chains of repeated monosaccharide units joined together by glycosidic bonds. Polysaccharides contain at least ten monosaccharide units and can be branched or linear chains. They are used in the storage of energy in the form of starch in plants and in the form of glycogen in animals and fungi. In addition, polysaccharides act as structural components in plants as cellulose and in arthropods as chitin.[2]

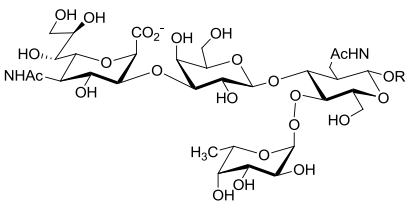

Sialyl Lewis a (sLe^a)

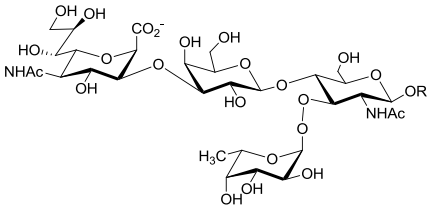

Sialyl Lewis x (sLe^x)

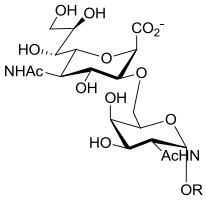

Sialyl Tn (sTn)

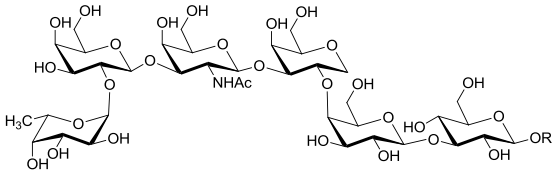

Globo H

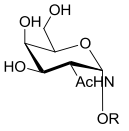

Tn

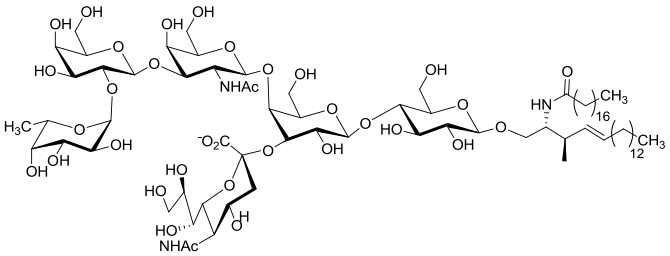

Fucosyl GM1

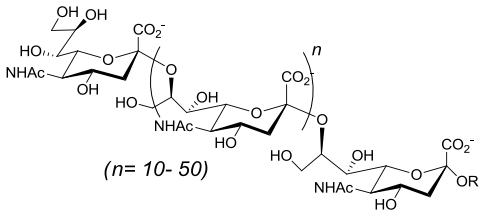

Polysialic Acid (PSA)

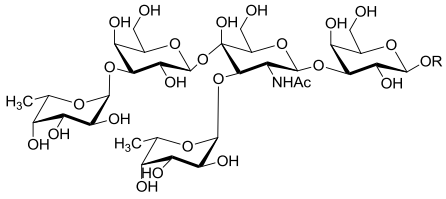

Lewis y (Le^y)

Figure 1.1 Physical structures of cancer-associated glycans

In living cells, most membrane-associated and secreted proteins contain appended carbohydrate structures, existing as glycoconjugates of different molecular configurations such as glycoproteins, glycosaminoglycans, and proteoglycans.[3] When cells are healthy, these various structures play important roles in molecular recognition at fertilization,[4,5] cell–cell interactions[6], protein degradation, and most crucially, in cell signaling.[7] However, in tumor cells, some of these glycans tend to be over-, under-, or newly expressed and these alterations can often make the tumor cells grow, divide and metastasize differently.[3] This phenomenon was first discovered by Meezan et al. in 1969 where they showed that there is a marked decrease of membrane sugars, especially sialic acid and *N*-acetylgalactosamine, following SV-40 virus transformation.[8] This abnormal expression in glycosylation is found in cancer[9,10], retrovirus infection,[11,12] and other diseases[13]. Another feature of tumor cells is the aberrant production of certain glycolipids and glycoproteins. In epithelial tumors, mucin glycoproteins, which contain dense clusters of *O*-linked glycans, are often overproduced. As such, mucins are used as diagnostic markers of cancer and can serve as scaffolds for most of the cancer-associated glycans shown in Figure 1.1.[14] In addition, cancer cells can overexpress gangliosides, which are glycosphingolipid-containing sialic acids. For example, complex gangliosides such as GD2, GD3, and fucosyl GM1, as shown in Figure 1.1, are shown to be overproduced in small-cell lung carcinomas, neuroblasts and melanomas.[15] Although it is apparent that tumor cells have aberrant glycosylation, there is no one single change that distinctly differentiates normal and malignant cells.

Table 1.1 Expression of cancer glycans on malignant tissues[16,17]

Cancer Glycan	**Malignant Tissue**								
	Ovary	Pancreas	Blood	Breast	Colon	Brain	Prostate	Skin	Lung
sLe^x		X		X	X				X
sLe^a		X		X	X				X
sTn	X	X		X	X		X		X
TF	X			X	X		X		
Le^y	X	X		X	X		X		X
Globo H	X	X		X	X		X		X
PSA		X	X	X		X			X
GD2			X			X		X	
GD3						X		X	
Fucosyl									X
GM2	X	X	X	X	X	X	X	X	X

Each type of cancer tissue is defined by a set of variation in glycan expression as shown in Table 1.1. For example, sialyl Lewis X (sLe^x) is associated with the metastasis of B16 melanoma cancer;[18] carbohydrate ligand binding to E-selectin controls the extravasation of cancer cells and organ selectivity of metastasis;[19] sialyl Lewis a (sLe^a) binding to selectin and is involved in the extravasation of human colorectal carcinoma cells;[20] endothelial cell adhesion, often controlled by carbohydrate–selectin binding, is correlated with cancer metastasis;[21] and the presence of sLe^a on cancer cells is correlated with risk of cancer metastasis.[22] This occurrence is medically significant as it highlights opportunities for therapeutic and diagnostic approaches[23].

As discussed above, glycans tend to be over-, under-, or newly expressed in tumor cells. These changes often arise due to the altered glycosyltransferase levels in cancerous cells, which modifies the core structure of *N*-linked and *O*-linked glycans. Glycosyltransferases, enzymes that form the glycosidic bonds between sugar units, produce an increased enzyme level that often results in an increase in the size and brancing of *N*-linked glycans that in turn cause an increase in global sialylation.[24] In addition to changes in the glycan core structure, modifications of the terminal structures are also linked to diseases. In tumor cells, glycosyltransferases involved in linking terminating residues on glycans are more active leading to overexpression of certain terminal glycans. Common examples of these terminal glycan epitopes displayed on malignant cells are sialyl Lewis X (sLe^x), sialyl Tn (sTn), Globo H, Lewis Y (Le^y) and polysialic acid (PSA)[10,15a,25] as shown in Figure 1.1. These glycans are present in malignant tissues in the brain, breast, colon, and prostate etc. as shown in Table 1.1.[26]

A vital technique in the detection of these glycoproteins in diagnostics is the immunoassay for carcinoembryonic antigen (CEA). CEA, a tumor-associated mucin antigen, was first described as a colon cancer marker in 1965 by Gold and Freedman.[27] When isolated, CEA is a glycoprotein consisting of ~60% carbohydrate and a molecular mass of ~180–200 kDa.[28] Most of the carbohydrate is composed of mannose, galactose, *N*-acetylglucosamine, fucose, and sialic acid.[28] CEA levels in mammalian systems are helpful in monitoring response to treatment and in determining whether there is possibility of relapse. The CEA test monitors serum levels of an antibody specific for a cancer-associated glycan, sLe^a.[29] In addition to colon cancer, it is also used as a marker for other forms of cancer, including cancers of the rectum, lung, breast, liver, pancreas, stomach, and ovary. Elevated levels of CEA in the blood exhibit a strong, positive correlation with an increased risk of relapse and metastasis. The CEA test is used to monitor CEA levels in colon cancer patients, and although it has proven to be valuable, tests like these have their drawbacks because they are unstable towards rigorous use, expensive, and difficult to produce. Other serum markers, such as CA125[30] and prostate-specific antigen,[31] reveal aberrant glycosylation in ovarian and prostate tumor tissues. However, for many cancers, there are no serum markers and the tissues must be analyzed directly. Existing methods requires surgical biopsy of tumor tissue followed by histological analysis with lectins and monoclonal antibodies. Hence, viable alternatives for detection of glycans are being actively pursued.[32]

An interesting future direction to detect aberrant glycosylation is by using probes for image contrast.[33] As mentioned above, mucin glycoproteins are overproduced in

epithelial tumors. Specifically, underglycosylated MUC1 antigen (uMUC1) is highly overexpressed in various human epithelial cell adenocarcinomas and is an early marker of tumorigenesis.[34] The protein portion of uMUC1 can be recognized by a specific peptide (termed EPPT1) derived from a monoclonal antibody.[35] Epenetos and co-workers developed an EPPT1 based probe that is capable of monitoring breast cancer *in vivo*.[35b] More recently, Dai and co-workers synthesized an EPPT1 conjugate that can be used for magnetic resonance and optical imaging.[36] Experiments with this new probe showed promising results as positive tumor models showed accumulation of probe in the tumor tissues while there was very low signal in uMUC-1-negative tumors. However, uMUC1-specific imaging targets the underglycosylated protein, not the carbohydrate directly.

This thesis describes work towards developing a method that would allow for effective detection of glycans. Boronic acids are known for forming strong, reversible, covalent bonds with 1,2 and 1,3 *cis*-diols on many sugar molecules.[37] These boronic acids-based lectin mimics are cheap, easy to synthesize and stable towards rigorous use. Hence, we believe that they can be used as lectin mimics to detect aberrant glycosylation in a small molecule microarray, which will be discussed in further detail in Section 1.3.

1.2 Types of Receptors and Sensors for Saccharide Binding

Receptors and sensors for carbohydrate binding can be classified into four categories: (1) antibodies,[38] (2) lectins,[39] (3) aptamers based on nucleic acids,[40] and (4) small molecule lectin mimics.[41] Antibodies are traditionally used in the recognition of a

litany of analytes including carbohydrates. However, they are not used in large-scale arrays due to cost and stability. Currently, lectins are the most available tools used in research for carbohydrate recognition but they often have issues with cross-reactivity.[42] Hence, it is important to develop new alternatives that possess: (1) high affinity, (2) high specificity, and (3) are suitable for high throughput analysis. This allows for accurate and precise study of carbohydrate changes at the glycome level. In order to fulfill these requirements, there have been major recent developments in fluorescent sensing methods for carbohydrates for a variety of applications. To this end, small-molecules and “polymeric binders” have been actively developed. One significant example is the use of boronic acid-based carbohydrate sensors, such as boronolectin, which is a specific term for peptides containing boronic acids. There are small molecule boronolectins (SBL), peptidoboronolectins (PBL), and nucleic acid-based boronolectins (NBL).

The first phenylboronic acid (PBA) was synthesized by Michaelis and Becker in 1880.[43] However, it was 74 years before scientists discovered the ability of boronic and boric acid to bind with diols. Later publications detailed the studies of a variety of diols and their binding interactions with boronic and boric acid[44,45]. In 1954, Kuivila and his co-workers noticed that polyols and saccharides were soluble in boronic acid solutions, and they suggested the formation of a cyclic ester.[46] This result agreed with the known ability of borates to interact with hydroxyl compounds. It was in 1959 that Lorand and Edwards reported the first quantitative study of the binding constants between several compounds containing diols and PBA.[47]

Boronic acids have been known to form strong and yet reversible covalent bonds with 1,2- and 1,3-substituted Lewis base donors such as hydroxyl, amino, and carboxylate groups. This interaction with diol or alcohols results in boronic esters (neutral trigonal boron) or boronate esters (anionic tetrahedral boron) based on the oxidation state of the central boron atom. All these properties have been studied and explored extensively in research as it allows for boronic acid compounds to be used as lectin mimics, as nucleotide and carbohydrate transporters, and as affinity ligands for the separation of carbohydrates and glycoproteins.[48] As shown in Figure 1.2, the boronic acid (**1**) has an empty boron orbital that allows for reaction with a protic solvent to form an anionic tetrahedral boronate (**2**) with the release of a proton. Upon reaction with the diol moiety, the boronic acid is converted into a boronic ester (**3**), which is similar to boronic acid because it can react with a water molecule, release a proton, and become a boronate ester (**4**). The equilibria for the formation of the anionic boronate complex is defined as K_{tet}, and the formation of a boronic acid complex is defined as $K\text{t}_{rig}$. In general, binding with a diol lowers the pK_a of the boronic acid.[37]

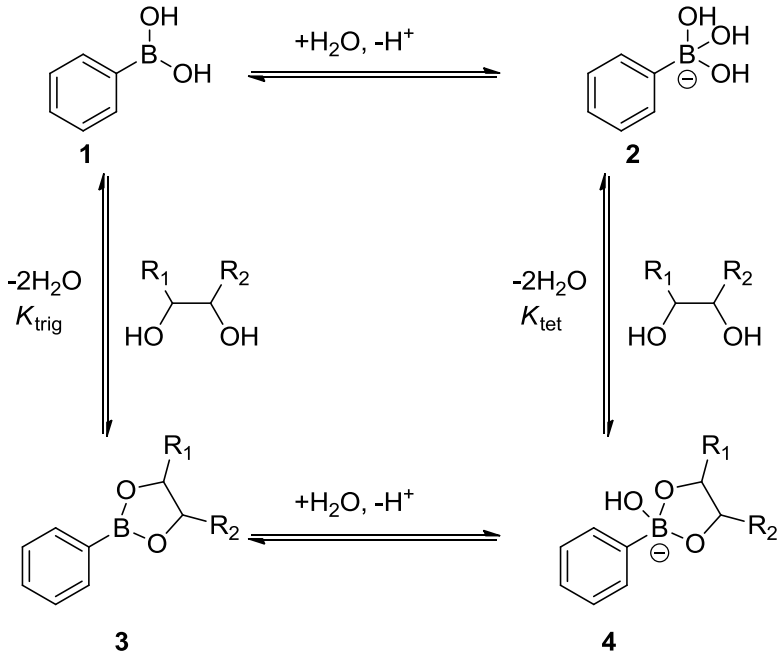

Figure 1.2. Binding of phenylboronic acid with a diol

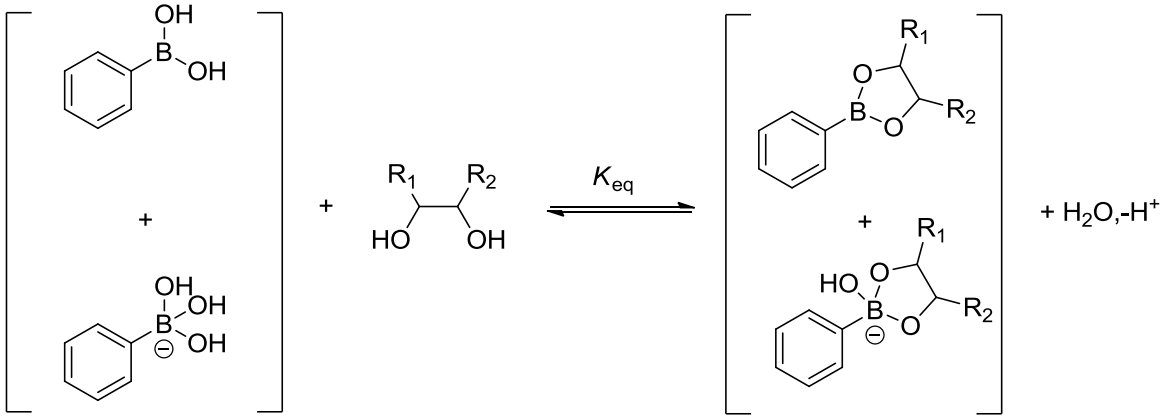

Figure 1.3. Overall binding of phenylboronic acid with a diol

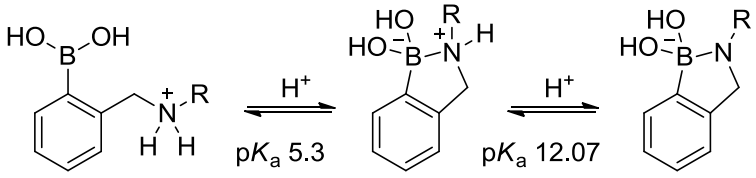

Figure 1.4. Equilibria for *ortho*-aminomethylphenylboronic acids

The binding of boronic acids to diols can be interpreted one of two ways. One way is to look at individual chemical reactions and the binding between the trigonal boronic acid and the diol or the binding between the tetrahedral boronate and the diol as shown in Figure 1.2. In this case, K_{trig} represents the binding constant between the trigonal boronic acid and the boronate ester; and K_{tet} shows the equilibria between the tetrahedral boronate and the boronate ester anion. The binding of boronic acids can also be described in Figure 1.3, which shows the overall binding equilibria instead of the individual reactions. In this case, K_{eq} is used to describe the overall binding constant, which is an apparent binding constant but is directly relevant to the equilibrium between a sensor and a carbohydrate.

In order to develop a practical boronic acid-based carbohydrate sensor, it is vital that binding can occur at physiological pH. However, since the reported pK_a of phenylboronic acid is 8.8, a design to lower the pK_a of boronic acid is necessary for strong binding to occur. B–N bond formation, when functionalized in a relative 1,5 position, acts as a special boronic acid-based sensor, as was shown by the work of Wulff[49] and Shinkai.[50] Wang and co-workers have studied in detail how the B–N bond changes in character as it forms complexes with carbohydrates.[51] These results were further supported by structural work from the Anslyn lab.[52] A method, developed by Wulff, used a neighboring aminomethyl group as shown in Figure 1.4. The pK_a for the second stepwise protonation in water of *ortho*-aminomethylphenylboronic acids was reported by Wulff[53] and Anslyn, Canary, and co-workers[54] to be 5.3.

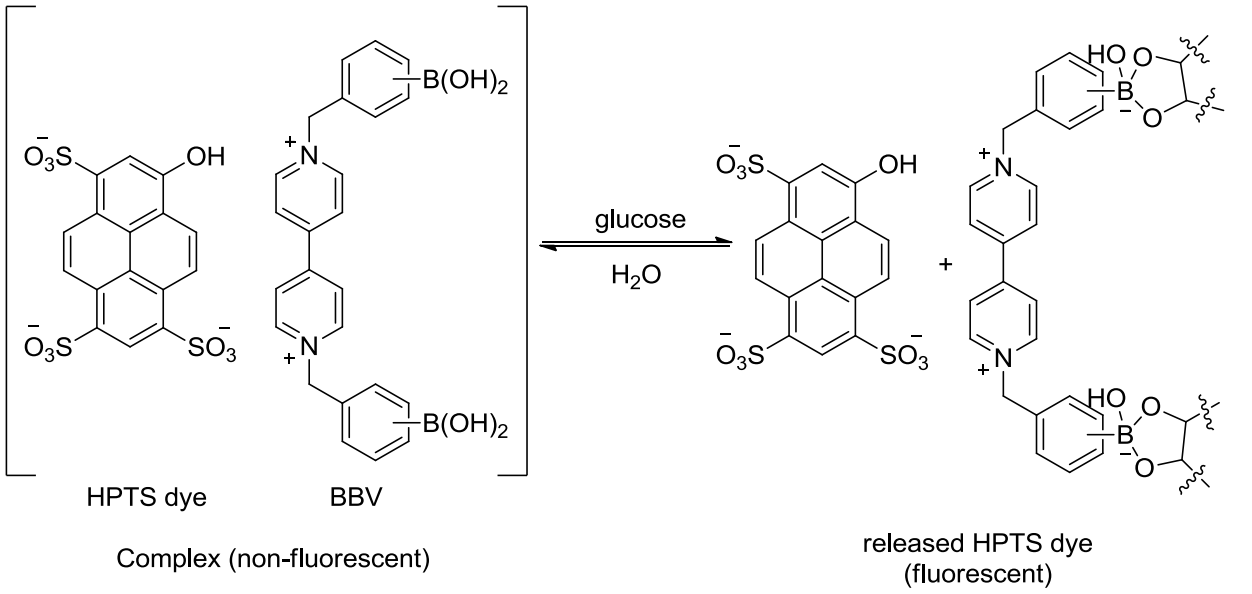

Figure 1.5. Mechanism of sugar sensing by the viologen–boronic acid system.

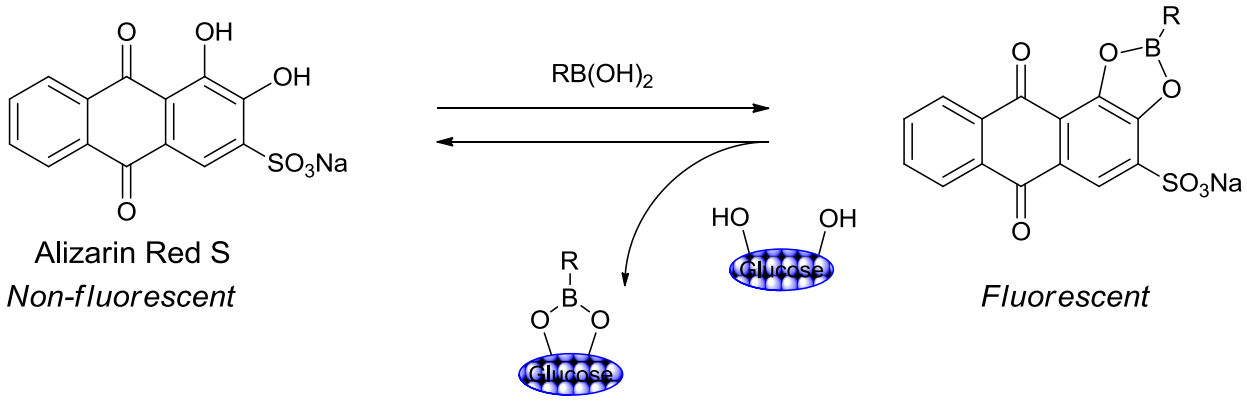

Figure 1.6. Dye displacement reaction of the adducts between boronic acid derivatives and Alizarin Red S (ARS) for glucose sensing.

Since boronic acids are able to react with diols and single hydroxyl groups, they are the most commonly used moieties for the construction of binders for carbohydrates, which contain many hydroxyl groups. One of the most common techniques employed is

the use of fluorescent sensors. An example of a small molecule boronic acid sensor for saccharide is the viologen bisboronic acid system developed by Singaram and co-workers.[55] The system uses anionic fluorescent dyes in combination with boronic acid as a chromophore and a recognition unit. Viologen is a dye that is considered to be electron deficient and redox sensitive. A mixture of substituted viologen boronic acid and fluorescent anionic dye solution results in a nonfluorescent complex due to stacking and quenching presumably due to charge transfer.[55b] Once bound to a sugar, the boronic acid moieties are converted to their anionic form, which combined with the bulkiness of the molecule results in dissociation of the nonfluorescent complex and triggers an increase in fluorescence intensity as shown in Figure 1.5. The sensitivity of the system can be adjusted by modifying the ratio of the anionic dye 8-hydroxypyrene-1,3,6-trisulfonic acid trisodium salt (HPTS) and the boronic acid-substituted benzyl viologens (BBV) recognition unit.

Another example of fluorescent sensors is the use of alizarin and its derivatives.[56] A displacement of binding between boronic acid derivatives and diols containing fluorescence dyes such as alizarin or Alizarin Red S (ARS) by a target saccharide as shown in Figure 1.6, which has been used to develop new sensors.[57] Alizarin and their derivatives normally provide a very weak emission and their fluorescence intensities are turned on when forming adducts with boronic acids. When diol-containing compounds are added into the alizarin-boronic acid mixture, the alizarin derivatives are displaced and the fluorescence signals are turned off. The decreasing

degree of fluorescence intensity depends on the concentration of the diol-containing compounds added.

Recently, there has been more interest in the design of nanoparticulate materials since they were found to have several advantages owing to their small size and high surface-to-volume ratio.[58] Larpent and co-workers developed a system of boronic acid-functionalized nanoparticles for use as a re-usable optical nanosensor for carbohydrates.[59] It is believed that boronic acid-functionalized nanoparticles can possibly provide valuable supports for the optical detection, the transport, or the separation of carbohydrates. They reported on the synthesis of boronic acid functionalized nanoparticles and the study of their diol binding capacity. The catechol, ARS, and the boronic acid-functionalized nanoparticles afford an optical colored nanosensor. This nanosensor is then used for fructose binding and detection in a competitive assay. As mentioned earlier in the section, the binding of sugar is evidenced by a color change. The boronic acid functionalized nanoparticles are formed by reacting 3-aminophenylboronic acid (APBA) with NL-CH_2X at room temperature, as shown in Figure 1.7. The nanosensor allows the visual detection of fructose as shown in Figure 1.8. The binding of fructose to boronic acid-functionalized nanoparticles is easily observed by the color change of NL–$B(OH)_2$–ARS mixture from orange to burgundy due to released ARS. When titrations were performed with increasing concentrations of fructose, it was evident that the ARS was being displaced with fructose due to the absorbance change. However, when the same titration was performed with glucose, it does not perturb the ARS-supported boronic acid equilibrium even at high

concentrations. Due to this interesting phenomenon, Lapert and co-workers went on to discover applications for the boronic acid-functionalized nanoparticles as it allows for selective separation of fructose from mixtures.

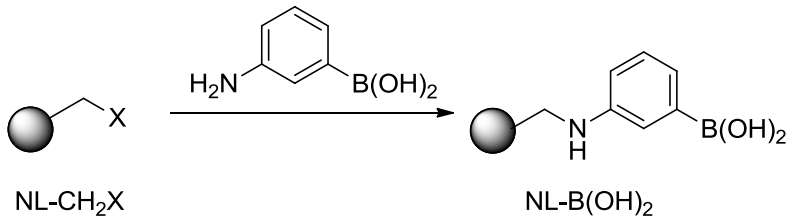

Figure 1.7. Preparation of boronic acid-funtionalized nanoparticles

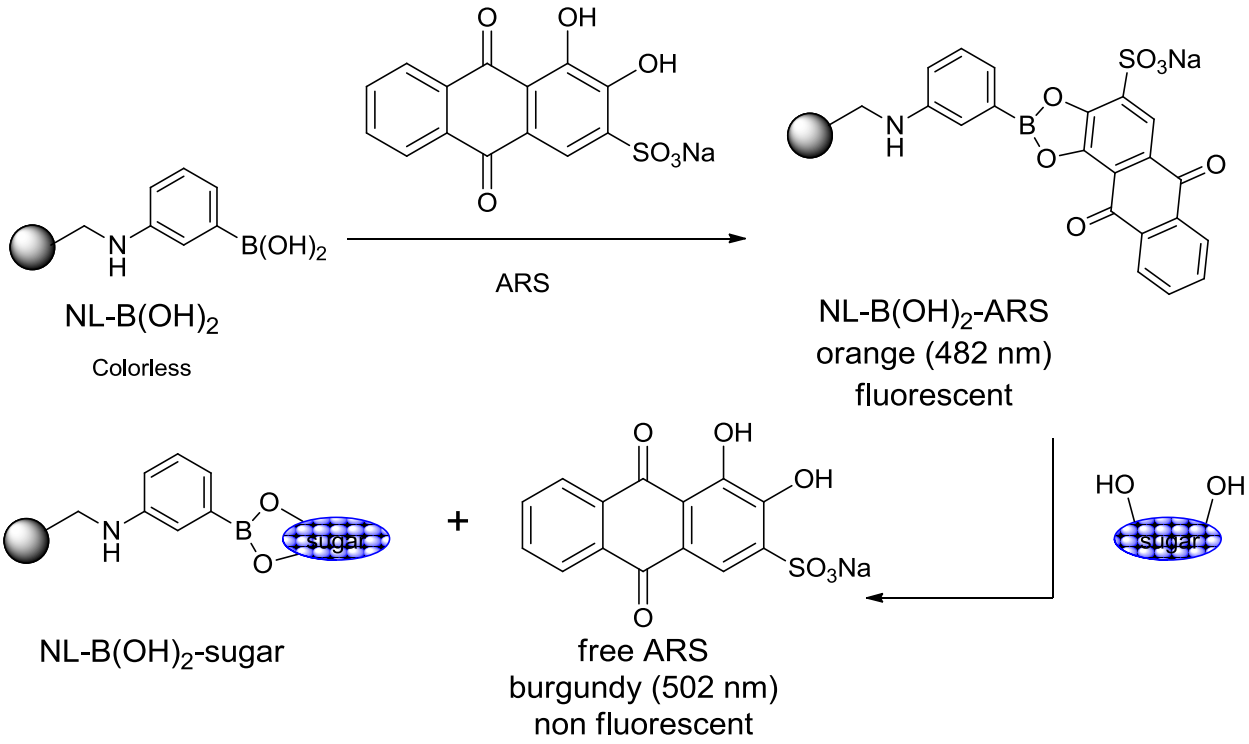

Figure 1.8. Competitive assay: binding of the dye (ARS) and dissociation in the presence of a carbohydrate.

1.3 Microarray Analysis of Binding between Boronic Acids and Glycoproteins

Over the past two decades, microarray analysis has transformed the life science research landscape. Microarray is a technique that can screen multiple reagents simultaneously with minimal consumption of sample. Essentially, it is a multiplex lab-on-a-chip. An example of a scanned microarray slide with a fluorescence intensity gradient is shown in Figure 1.9. The technology itself was first used in DNA assemblies on chips, but shortly thereafter, it was possible for researchers to sequester small molecules[60] and then proteins[61] for rapid analysis. By now, microarray technology has progressed to the point where we can examine a host of other biomolecules, including membrane proteins,[62] carbohydrates,[63,64] and peptides,[65] as well as complex structures such tissues[66] and even live cells[67] on arrays. It is noteworthy how a single technology platform has developed for so many diverse applications. In comparison to microtiter-based assays, microarrays are high-throughput and offer a flat surface for the washing and incubation steps. This design concept makes it possible to process thousands of assays quickly and in a less costly manner by reducing the amount of expensive reagents required.

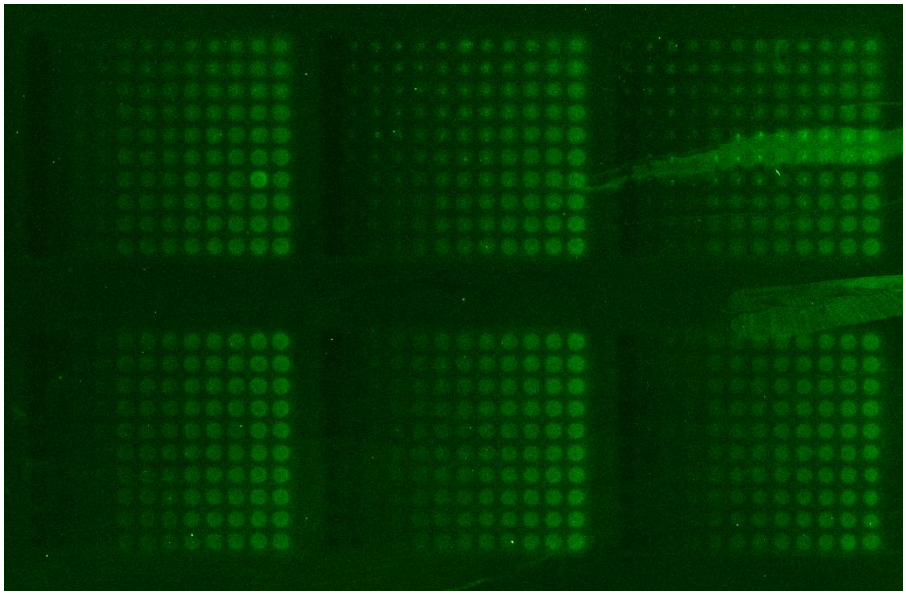

Figure 1.9. Image of scanned microarray glass slide with fluorescence intensity gradient

Microarrays can be classified into two general types, biochips (biomicroarray) and chemical microarray (small molecule microarray).[68] Biochips are arrays of biological components, such as protein, DNA, cell, and tissue. Chemical microarrays are arrays of organic compounds including small organic molecules, peptides, and sugars. In 1999, MacBeath and Schreiber published the first small molecule microarray research. They immobilized thiolated compounds onto maleimide-derivatized slides through a thioether bond and screened them against a series of model proteins.[60] Chemical microarrays have a wide variety of applications, ranging from drug and biomarker discovery to disease detection and profiling.[69] For example, chemical microarrays are used in modern drug discovery research to study the interaction between small molecules and biological targets.[70] Figure 1.6 shows the interaction of amino-modified DNA with an epoxysilane glass slide from Schott Nexterion®.

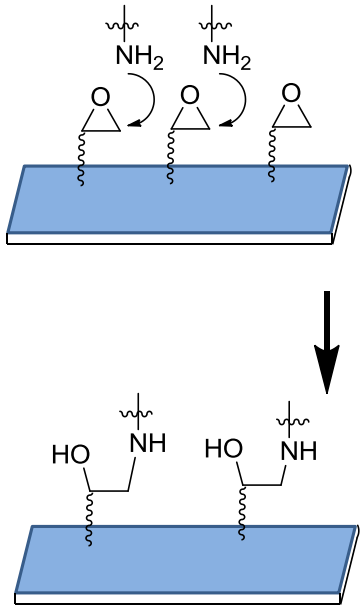

Figure 1.10. Immobilization chemistry of primary amine to epoxysilane glass slides

As compared to DNA and protein microarrays, the development of chemical microarrays has progressed more slowly.[71] One reason for this is that, unlike certain biomicroarrays, there is no general linking technology that can be applied to immobilize different compounds containing different functional groups on the same glass slide. A litany of strategies has been developed to fabricate chemical microarrays. For example, stable carbohydrate microarrays can be fabricated using Michael addition,[72] Diels–Alder reaction,[73] Staudinger ligation,[74] click chemistry,[75] Schiff base formation,[76,77] and amide bond formation.[78,79] The detection methods for microarray has matured and extended beyond fluorescent labels, to include label-free optical impedance measurements,[80] surface plasmon resonance[81] and mass spectrometry-based techniques.[82] Lin and co-workers developed a novel and straightforward carbohydrate microarray through boronate formation.[83] Boronic acid forms a stable but reversible complex with *cis* 1,2- or

1,3- diols of carbohydrate, and this allows it to be used as a glycol-targeting probe in numerous applications.[48a, 48f, 84] They reported the use of an aldehyde-functionalized slide that was reacted in solution to produce a boronic acid-functionalized slide that would provide a simple and straightforward way of attachment of a litany of unmodified carbohydrates onto the slide surface. The carbohydrates were then probed with biotin-labelled lectins or antibodies and then detected by Cy3-streptavidin or Cy3-conjugated secondary antibodies. 3-Aminophenyl boronic acid (APBA), a cheap and readily available boronic acid was selected to implement the carbohydrate microarray. This developed method is suitable for all sizes of carbohydrates besides monosaccharides. The reason is that the hydroxyl groups involved in lectin recognition could be occupied by the boronic acid. This method is highly convenient as it circumvents the modification of sugar molecule before immobilization which is often tedious and time consuming.

Another notable strategy in glycomics, i.e. the high throughput analysis of carbohydrates, is the use of lectin microarrays.[85] Lectin microarrays are a form of protein microarray that utilizes glycan-binding proteins that have proven to be very effective for the high-throughput analysis of glycans.[86] However, the majority of lectins being used are proteins isolated from plants. These plant lectins are isolated and purified from natural resources, which often result in inconsistent activity and availability due to differences in purification and seasonal changes. In addition, most plant lectins exist as glycoproteins so the lectins themselves could serve as receptors for carbohydrate-binding proteins leading to false positives. To resolve these issues, Mahal and co-workers set out to create a recombinant lectin with bacterially- derived lectins for

use in microarray technology.[85] They cloned, expressed and purified a small panel of lectins as N-terminal GST–His_6 fusions with no noticeable effects on specificity and provided the possibility of an oriented microarray. In microarray analysis, the simple lectin panel was able to distinguish between both glycoprotein samples and cell lines, supporting the idea that a broader lectin panel may be useful for both diagnostics and carbohydrate analysis. This technology is highly efficient as it allows for rapid assessment of carbohydrates using minimal sample amounts (<1 μg).[86] By standardizing the conditions for cloning, expression, and purification of bacterial lectins, it is possible for us to create a large, well-defined lectin library for the rapid analysis of complex carbohydrates.

1.4 FRET-Based Detection

In addition to microarray technology, detection using Förster Resonance Energy Transfer (FRET) is also often used the study of carbohydrates. In order to characterize and detect the density of glycosylated surfaces, an efficient method is needed that offers high resolution in identifying clusters of dense glycans on cell surfaces. This is useful in lipid rafts because cell membranes have regions that are concentrated with specific components, such as sphingolipids, that result in areas of dense glycosylation.[87] These regions have high signaling activity in cells, and it is important that they be characterized. To this end, we designed carbohydrate binding boronic acid receptors derivatized with FRET.[88]

FRET is commonly applied in biology and chemistry and has been used to measure distance and detect molecular interactions in a number of systems. In this

sense, FRET has been used to provide information about protein conformation because it measures distances between domains in a single protein.[89] Applied in vivo in living cells, FRET has given us the opportunity to explore the location and interactions of genes and cellular structure such as integrins and membrane proteins by using variation of the Green Fluorescence Protein (GFP).[90] In addition, FRET can be used to obtain information of crucial biological pathways and is also used to study lipid rafts in cell membranes.[91]

FRET describes the energy transfer between two fluorophores. This mechanism was first discovered by the German scientist Theodor Förster in 1948.[92] When employing FRET, a donor and an acceptor are involved. When a donor fluorophore is excited, it transfers energy to an acceptor in close proximity, and this allows for the transfer of energy through nonradiative dipole–dipole coupling as shown in Figure 1.11. When choosing FRET pairs, it is a requirement that the emission spectrum of the donor overlaps with the absorption/ emission spectrum of the acceptor. FRET can be an accurate measurement of proximity at very short distances (10–100 Å) and highly efficient if the donor and acceptor are within the Förster radius, which is typically 3–6 nm.[93] The technique itself is very sensitive and provides high resolution because the rate of energy transfer of FRET is dependent on the inverse sixth power of the distance between the donor and acceptor. Thus, in domains of dense glycosylation, we would observe an increase in acceptor emission and decrease of donor emission.[94] In areas of sparse glycoslyation, there should be little to no background acceptor emission. Hence,

we expect to detect regions of heavy glycoslyation with high resolution by using this FRET-based assay.

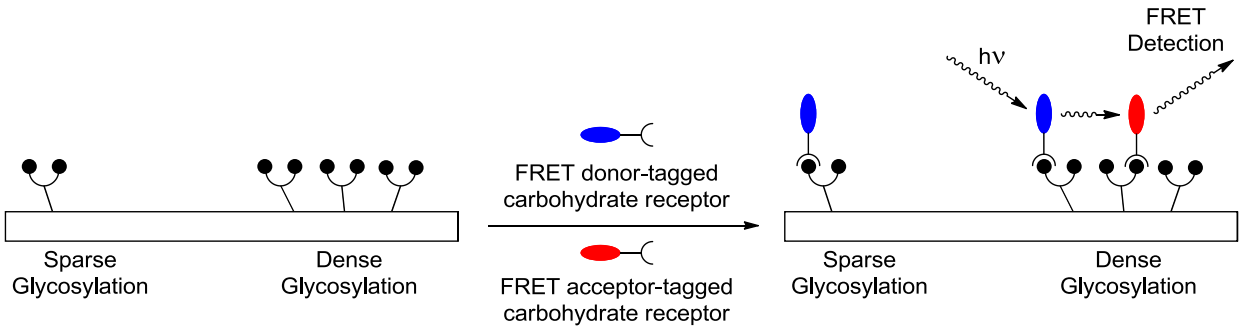

Figure 1.11. FRET-based assay for the detection of carbohydrate clustering on surfaces.

Chapter 2: Design and Synthesis of a Boronic Acid Lectin Mimic to study Carbohydrate Binding using Microarray Analysis and FRET

2.1 High-throughput Microarray Analysis

2.1.1 Research Design

In pursuing a boronic acid-based carbohydrate sensor, compound **2.3** (Figure 2.4), that is effective for microarray analysis, certain characteristics had to be incorporated. First, the final compound must have a terminal amine to cleave open the epoxides on the microarray glass slide to allow for attachment to the glass surface. Next, a phenylboronic acid is needed to facilitate binding to polyol compounds. An ethylene diamine linker was included to extend the distance between the boronic acid and the terminal amine. The aminomethyl group attached to the phenylboronic acid lowers the pK_a of the phenylboronic acid and allows for better binding at physiological pH.[49a]

Three different polyol compounds with fluorescent capabilities were selected for microarray analysis with boronic acid-based sensors: alizarin, tetramethylrhodamine tagged avidin, and mucin. Alizarin, or 1,2-dihydroxyanthraquinone, was used as a model to detect binding between catechols and boronic acids as catechols are known to have higher binding affinities as compared to sugars.[95] Upon binding with boronic acid moieties, alizarin becomes fluorescent as shown in Figure 2.1 and allows for direct detection of fluorescence.[96] Alizarin is an efficient model as it is cheap and commercially available. The microarray analysis results provided us with a range of concentrations of boronic acid-based sensors where we believe the fluorescence intensity to be

representative of binding between the sensor and catechol. Glycoproteins such as avidin and mucin were chosen to detect binding between sugars and boronic acids. Binding of avidin and mucin to slide surfaces for detection are shown in Figure 2.2 and 2.3. Glycoproteins were selected instead of simple sugars because they offer the option of multivalent binding sites. Generally, a glycoprotein contains many glycan chains and numerous kinds of carbohydrates. For example, Mucin1 (MUC1) is a glycoprotein with extensive *O*-linked glycosylation of its extracellular domain and contains sialic acid.[14] Hence, the boronic acid-based sensor on the slide surface would have multiple opportunities to detect the glycoprotein.

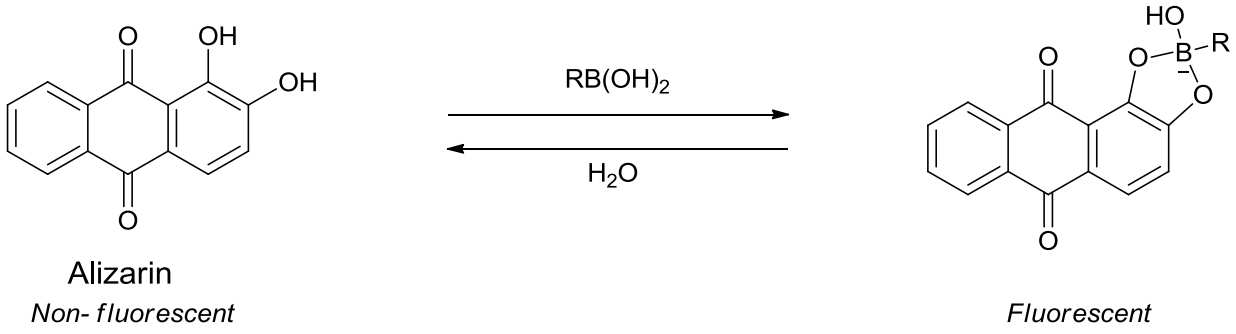

Figure 2.1 Binding of a boronic acid with alizarin and a 1,2-diol

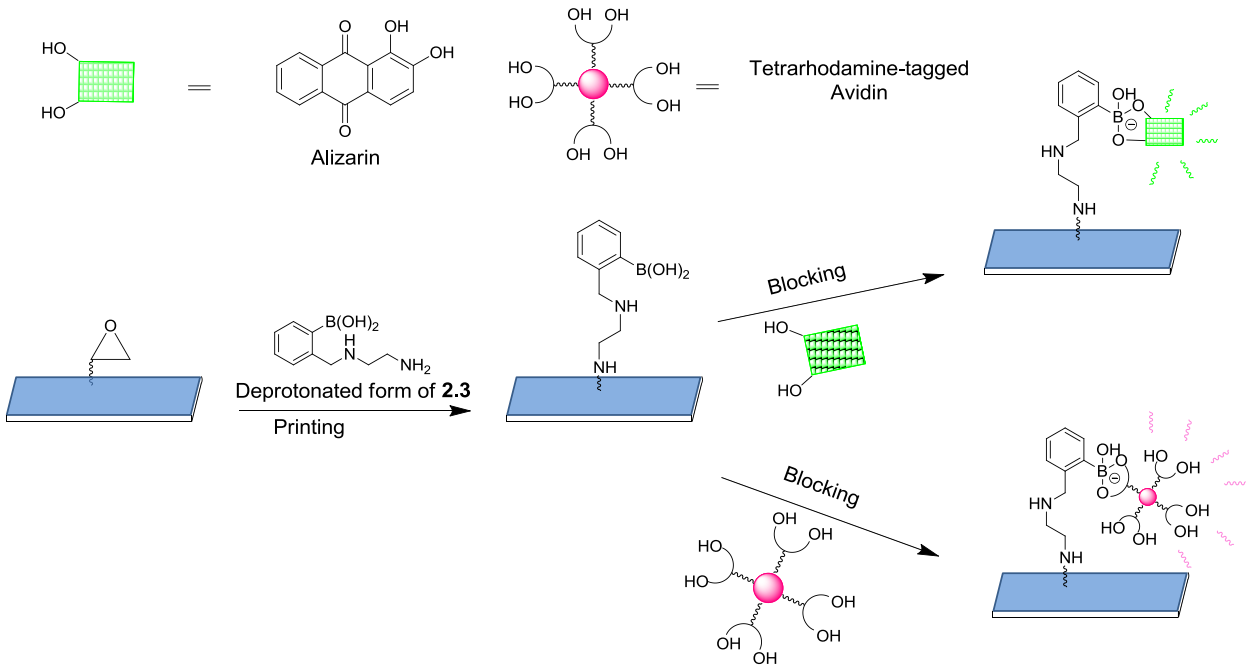

Figure 2.2. Binding of alizarin and avidin to microarray slide surface

Following the recognition of alizarin, we explored the detection of tetramethylrhodamine-tagged avidin. This is essential as it gave us an opportunity to directly investigate the binding of the glycoprotein with the boronic acid-based sensor as shown in Figure 2.2. However, fluorophore-tagged glycoproteins do not exist in nature and to accurately depict the binding of glycoprotein with our boronic acid-based sensor, we selected mucin1 for microarray analysis. Mucins line the epithelial cells in the lungs, stomach, intestines, eyes and several other organs.[34b] Overexpression of MUC1 is often associated with colon, breat, ovarian, lung and pancreatic cancers.[97] Upon printing the boronic acid-based sensor on the microarray slide surface, we incubated the supergrids with the mucin1 glycoprotein. Unlike the tetramethylrhodamine-tagged avidin, mucin1 is not fluorescent and antibodies are needed for detection. As shown in Figure 2.3, the

primary antibody, MUC1 antibody, and secondary antibody, Cy3-tagged goat-anti-rabbit antibody, binds to the MUC1 glycoprotein and the fluorescence is then detected to affirm binding.

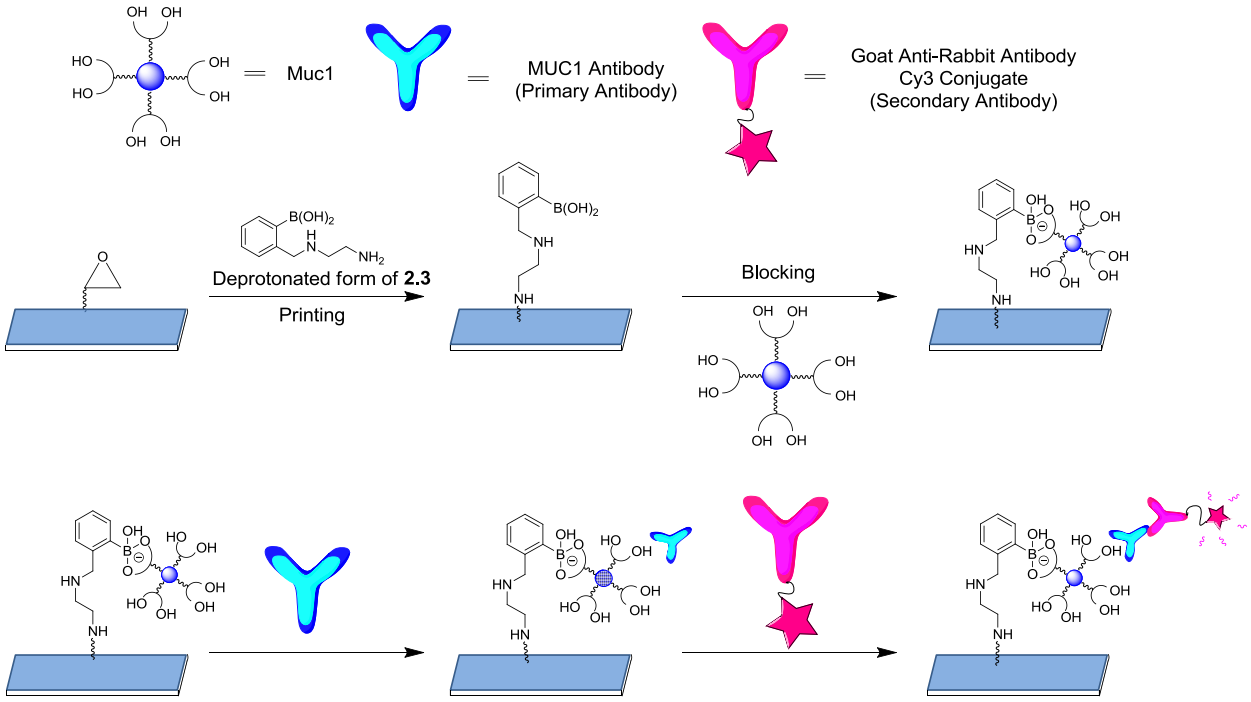

Figure 2.3. Binding of mucin1 to microarray slide surface followed by tagging with primary and secondary antibodies for detection

2.1.2 Research Synthesis of Compound 2.3

The final synthetic route to construct compound **2.3** is shown in Figure 2.4. It begins with the mono-Boc protection of commercially available ethane 1,2-diamine to produce compound **2.1**. The free amine is then coupled to 2-formylphenylboronic acid via a reductive amination to produce compound **2.2**. The Boc group was then deprotected by using trifluoroacetic acid to yield the trifluoroacetate-ammoium salt **2.3**.

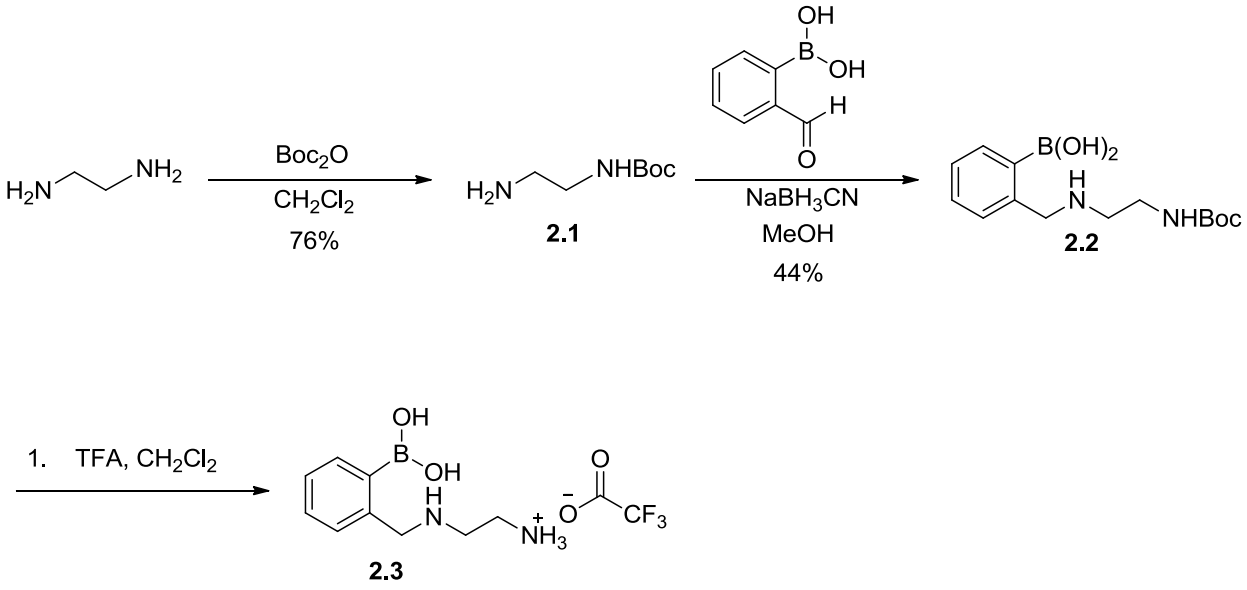

Figure 2.4 Synthesis of final product **2.3**

2.1.3 Results and Discussions

As mentioned above, boronic acids can form a stable but reversible complex with 1,2- and 1,3 diols of carbohydrate by formation of a boronate ester in aqueous media at room temperature.[47] Herein, we describe the utility of microarray analysis for using boronic acids as lectin mimics to detect certain carbohydrate structures. Compound **2.3** was printed onto epoxide-functionalized glass slides purchased from Schott Nexterion®. The amine of the ethylene diamine linker cleaves open the epoxides on the glass surface to form covalent bonds when immobilized with the basic print buffer (phosphate buffered saline (PBS), pH 8.5 and borate buffer, pH 9). On the slide, several supergrids are usually printed, and 12 different concentrations of each boronic acid will be on each supergrid. This is then followed by washing and blocking of the unreacted slide surface and then incubation with the polyol compounds.

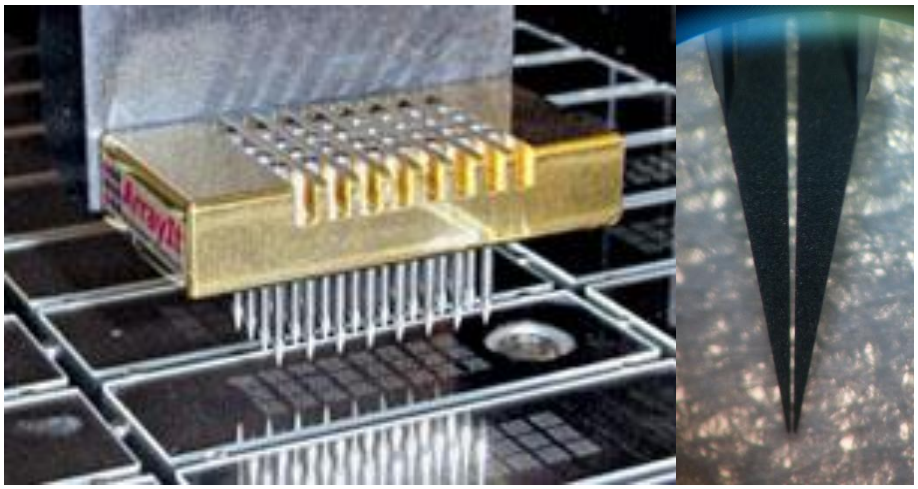

Figure 2.5 Left: Robotic pin printer holding 32 pins. Right: Close up image of a pin.

Using the SDDC-2 robotic printer from ESI, compound **2.3** was printed onto epoxide-functionalized glass slides. The pin on the robot has an uptake volume of 0.25 µL/ sample channel, a tip size of 75 µm, and a delivery volume of 600 pL. An image of the pin and printhead is shown in Figure 2.5. Several different buffers were used when spotting. We first attempted to use tris(hydroxymethyl)aminomethane (TRIS) buffer but that proved to be ineffective, and we postulated that the buffer contains a free amine group that could possibly compete with the boronic acid for reacting with epoxy functional groups. Borate buffer at pH 9 and PBS at pH 8.5 were tried out as print buffers and both provided reasonable results as shown in Figure 2.6–2.9. After overnight incubation, the printed slides were washed thoroughly to remove any unbound boronic acid. The slides spotted with borate buffer were washed with borate buffer containing 0.05% Tween-20 at pH 9 and the slides spotted with PBS would be washed with PBS with 0.05% Tween-20 at pH 8.5.

To avoid non-specific interaction between the diol moiety and the slide surface, it is essential to block the slide surface. Blocking was initially done with ethanolamine block buffer, but high fluorescence background was observed. Diethylamine block buffer showed better results and was used for subsequent assays. After an hour of blocking, the slide was washed thoroughly to remove any traces of block buffer and then dried. The slides spotted with borate buffer were incubated in a solution of buffered alizarin in methanol, and the slides spotted with PBS were incubated in a solution of alizarin in PBS. After alizarin incubation, the slides were washed thoroughly to remove any

unbound compound followed by detection of fluorescence by slide scanning.

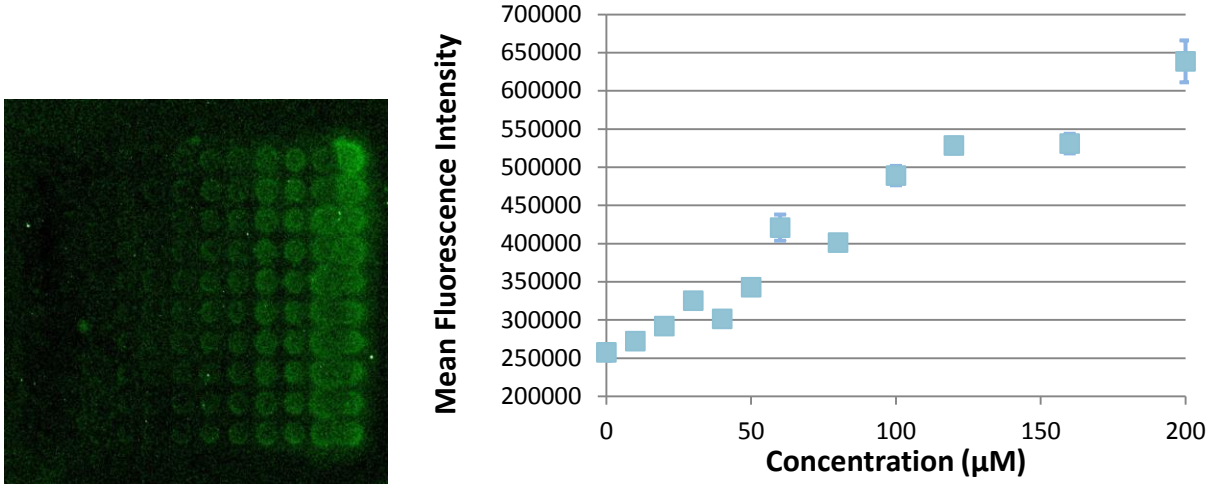

Figure 2.6 Left: Results of 0–200 µM compound **2.3** printed in 20 mM Borate buffer and 20% DMSO and incubated with 0.1 mM alizarin. Right: Graphed results of mean fluorescence intensity of each column on the left with error bars depicting the standard error.

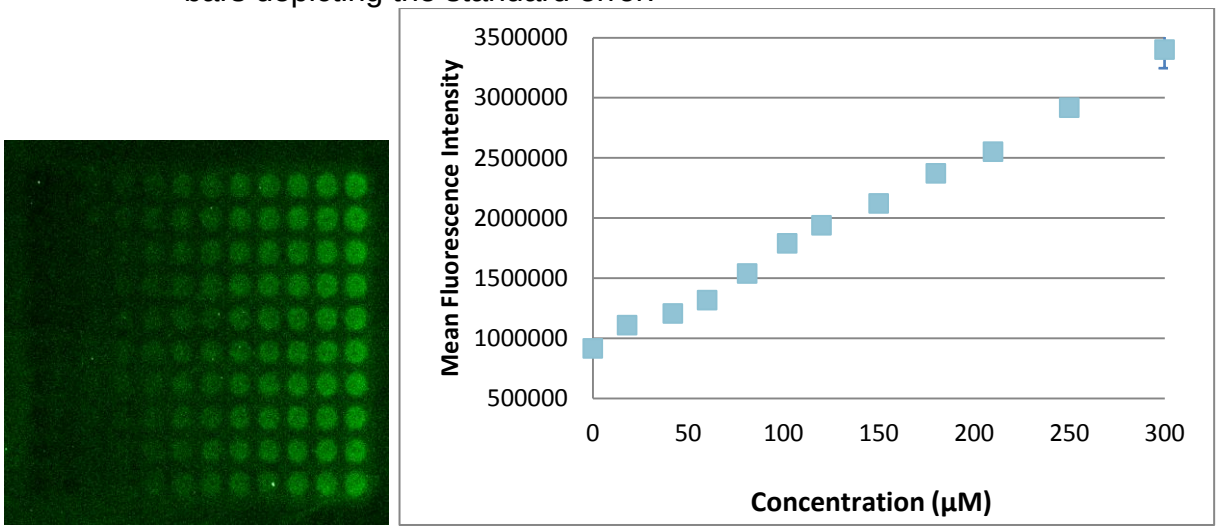

Figure 2.7 Left: Results of 0–200 µM compound **2.3** printed in 20 mM Borate buffer and 20% DMSO and incubated with 0.1 mM alizarin. Right: Graphed results of mean fluorescence intensity of each column on the left with error bars depicting the standard error.

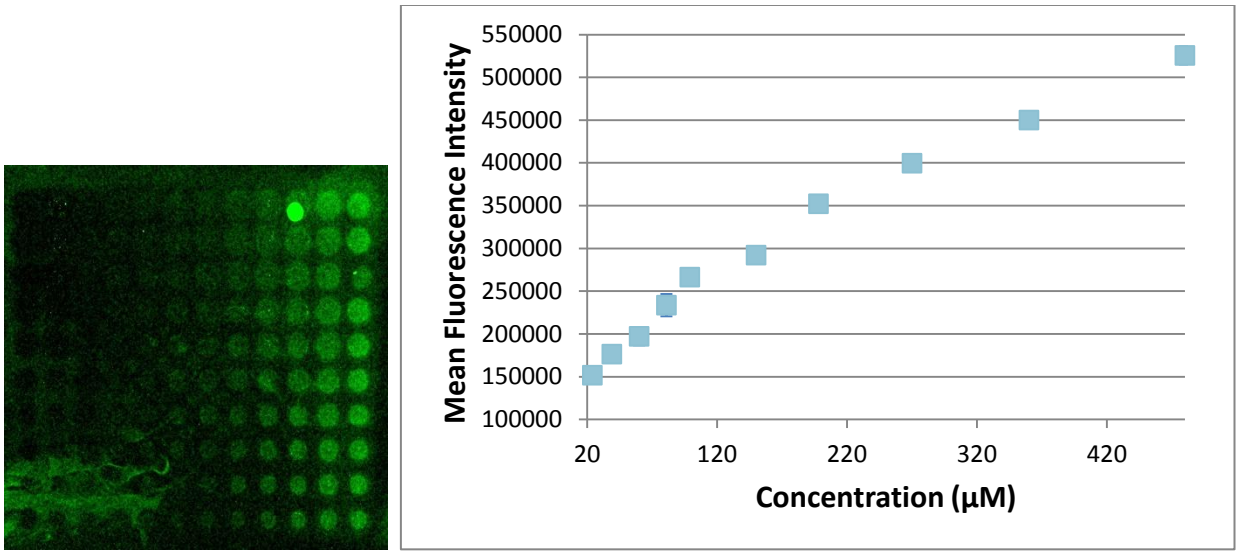

Figure 2.8 Left: Results of 0–480 µM compound **2.3** printed in 20 mM Borate buffer and 20% DMSO and incubated with 0.1 mM alizarin. Right: Graphed results of mean fluorescence intensity of each column on the left with error bars depicting the standard error.

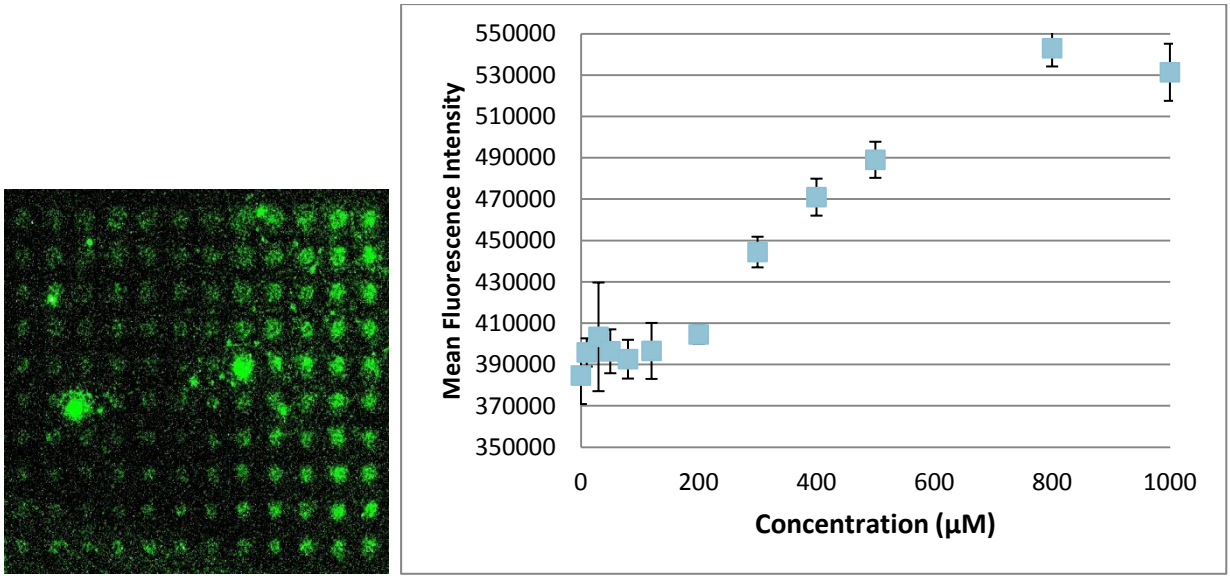

Figure 2.9 Left: Results of 0–1000 µM compound **2.3** printed in 30 mM phosphate buffer and 20% DMSO and incubated with 0.1 mM alizarin. Right: Graphed results of mean fluorescence intensity of each column on the left with error bars depicting the standard error.

Three different compounds with diol moieties were incubated with the boronic acid—alizarin, tetramethylrhodamine tagged avidin and mucin 1. Alizarin was used as a model for the fabrication of the microarray because catechols are known to have higher binding affinities with boronic acids than carbohydrates. Twelve different concentrations (0, 10, 20, 30, 40, 50, 60, 80, 100, 120, 160, 200 μM) of each boronic acid in 20 mM borate buffer with 20% DMSO were spotted on each supergrid, then blocked and incubated with its respective assay. The maximum concentration was initially capped at 200 μM as a previous study by Lin and co-workers observed plateauing of fluorescence intensity when the PBA concentration was at 200 μM. However, our results indicate that this maximum concentration does not apply to our assay.

Incubation with 0.2 mM alizarin in 20 mM borate-buffered methanol showed positive linear correlation between fluorescence intensity and concentration of boronic acid. The maximum boronic acid concentration used in printing was then increased to 300 μM, 480 μM, and ultimately to 1000 μM (300 μM and 400 μM were printed with 20 mM borate buffer at pH 9, and 1000 μM was printed with 30 mM PBS at pH 8.5) in order to achieve a plateau in fluorescence intensity. It was with printing up to 1000 μM that leveling off in fluorescence intensity was observed. Hence, 12 concentrations (0, 10, 30, 50, 80, 120, 200, 300, 400, 500, 800, 1000 μM) of boronic acids were chosen to be incubated with tetramethylrhodamine tagged avidin and mucin. Preliminary results with tagged avidin show that binding between avidin and PBA does occur because fluorescence spots were observed.

2.1.4 Conclusions and Future Work

We successfully used microarray techniques to show that binding between alizarin and boronic acid occurred on epoxide-functionalized slides. The printing of the boronic acid-based sensors proved to be the most challenging step in the microarray analysis. Ultimately, printing with 30 mM PBS with 0.05 % Tween at pH 8.5 proved to be effective. Blocking of the unreacted slide surface was initially unsuccessful with ethanolamine buffer but switching to diethylamine buffer rectified the issue. The slides were incubated with alizarin, tetramethylrhodamine-tagged avidin and MUC1 as shown in Figures 2.2 and 2.3. The work done with alizarin proved to be successful but the incubation of the boronic acid-based sensor with tetramethylrhodamine-tagged avidin and MUC1 requires further optimization.

Preliminary results of microarray analysis with tetramethylrhodamine-tagged avidin and MUC1 showed that the supergrids were visible, which is a positive indication of binding. However, unlike Figures 2.6–2.9 of the alizarin slides, a gradient of increasing fluorescence intensity was not observed. Hence, further optimization of the conditions is necessary.

2.1.4.1 Problems with Printing

Even though the previously mentioned microarray assays have yielded intital results, it could benefit from further optimization. One of the biggest problems we have faced with microarray analysis is inconsistency. The printing of samples on the slide surface has often proven to be temperamental. Typically, supergrids can be observed on the glass surface after printing as the printing buffer is an aqueous solution with high salt content. There are many instances where after printing, no visible spots can be

seen on the slide. If that is the case, no printing solution has been deposited on the slide surface. This could be due to many issues 1) The solution being spotted has evaporated before printing could occur, 2) The solution has clogged the pin tip, 3) The pin tip could be damaged. The evaporation issue can be addressed by increasing humidity of the environment while printing, adding high boiling and/or viscous solvents such as dimethyl sulfoxide or glycerol. In addition to having no spots, a frequent problem is pin clogging. It appears that during the printing sequence, the pin becomes clogged and stops depositing solution on the slide surface as seen in Figure 2.10b. This problem can usually be solved by adjusting the concentration of the buffer. For example, this phenomenon was a common occurrence when the printing buffer was 50 mM borate buffer with 0.05% Tween. Attempts were made to solve this problem by sonicating the pin before every print sequence and carefully air drying the pin, but it did not improve the printing situation. However, when we tried printing instead with 20 mM borate buffer with 0.05% Tween, the pin printed perfectly but the spots were hollow in the center. This could potentially cause inaccurate fluorescence readings. We postulated that this was because the printed spots were drying out too quickly, so new printing solutions with 20% DMSO were prepared to resolve this issue. At times, the spots printed could merge together as shown in Figure 2.10c. When this occurs, a simple solution such as adjusting the buffer concentration usually solves this issue.

Ultimately, if modifying the printing conditions does nothing to improve the printing situation, it is possible that the pin is damaged. A convenient way to determine whether the pin is damaged is to have it print solutions of printing buffers. If the pin is

able to print grids of buffers with no noticeable difficulty (clogging etc.), then further modifications should be made to the printing solution.

a) 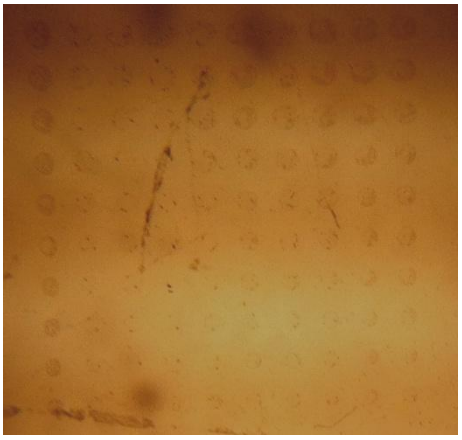 b)  c) 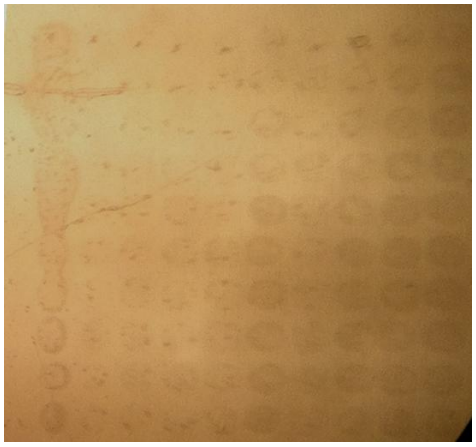

Figure 2.10. Image of supergrids as viewed under a microscope a) a well printed grid where spots appears to be evenly spaced and evenly sized b) a poorly printed grid where pin clogging occurs c) a poorly printed grid where spots merged together.

2.1.5 Experimental

Materials

Epoxysilane-coated glass slides (Nexterion slide E) were purchased from SCHOTT North America). Tetramethylrhodamine tagged avidin (Protein Mods), mucin 1, mucin 1 antibody and cy3 tagged goat-anti-rabbit antibody were purchased from Novus Biologicals; other standard chemicals were purchased from commercial suppliers and used as received. Glass slides were stored in a desiccator to keep them dry.

Methods

Microarray fabrication

Stock boronic acid solution was stored at 5 mM in water and kept at -20 ^{o}C in a freezer. When printing with borate buffer, 12 different concentrations (0, 10, 20, 30, 40, 50, 60, 80, 100, 120, 160, 200 μM) of boronic acids were prepared in a 96-well plate with 0 μM acting as the control. This was also repeated for printing up to 300 μM (0, 18,

42, 60, 81, 102, 120, 150, 180, 210, 250, 300 μM) and 480 μM (0, 9, 24, 39, 60, 81. 99, 150, 198, 270, 360, 480 μM). Initially, printing was done with 50 mM borate buffer but this clogged the pin, so the concentration of the buffer was lowered to 20 mM. However, after lowering the concentration of buffer, the spots appeared to be hollow, and that caused inaccurate fluorescence reading. We postulated that this was because the printed spots were drying out too quickly, so new printing solutions with 20 mM borate buffer with 0.05 % Tween at pH 9 and 20% DMSO were prepared. When printing with PBS, 12 different concentrations (0, 10, 30, 50, 80, 120, 200, 300, 400, 500, 800, 1000 μM) of boronic acids in PBS and 0.05% Tween at pH 8.5 were prepared in a 96 well plate with 0 μM acting as the control.

Using the standard robotic pin printer, the different solutions of boronic acids were printed on the epoxide-functionalized glass slides, and each super grid was printed in a 12 x 10 pattern. After an overnight incubation in a humidifying chamber, which is essentially a container holding a piece of hot paper towel, the slides were washed by submerging them in Petri dishes filled with wash buffer and gently shaking on a waver. The slides printed with borate buffer were washed with borate buffer and 0.05% Tween at pH 9, and the slides printed in PBS were washed with PBS buffer and 0.05% Tween at pH 8.5. The slides were washed 3 separate times with their respective wash buffer at 5 minute intervals. Blocking was done by gently shaking the slide on a shaker for 1 hour with the slide in a Petri dish filled with 20 mM diethylamine in 20 mM borate buffer and 0.05% Tween at pH 9. After blocking, the slides were washed three

times at 5 minute intervals with their respective wash buffers and then dried with nitrogen air and used for incubation.

Binding Assays

Alizarin was dissolved in borate-buffered methanol to give a concetration of 0.1 mM alizarin (borate buffer: 20 mM boric acid, 20 mM sodium borate in methanol at pH 8.5). During incubation, the glass slide would be submerged in 50 mL of buffered alizarin in a Petri dish for 1 hour. The Petri dish was covered to prevent evaporation of solvent. The Petri dish used for incubation was left on a flat surface and not placed on a waver as preliminary results showed that shaking provided unsuccessful results. After incubation was complete, the slides were washed 3 times with their respective wash buffer and 3 more times with water. Each wash with wash buffer took approximately 5 minutes and each wash with water took approximately 15 minutes. The slides were dried completely using nitrogen air and then scanned immediately to obtain results.

Data Analysis

Using the GenePix® 4000B microarray scanner from Axon instruments, the fluorescence intensities of microspots were quantified. The array reader has a 532 nm wavelength laser which scanned the slide and showed the image of the supergrid. The spot with no boronic acid was used as the control. The spots which showed anomalous results such as abrupt lower or higher fluorescence were removed from the analysis.

2.2 FRET Detection

2.2.1 Research Design

In order to characterize and detect the density of glycosylated surfaces, we set out to design carbohydrate-binding boronic acid receptors derivatized with FRET pairs as shown in Figure 2.11. To achieve this goal, several fluorophore-tagged boronic acids were synthesized by my co-workers and me. Coumarin-tagged (synthesized by me) and NBD-tagged (synthesized by Chí-Linh Đỗ-Thanh) boronic acids, **2.5** and **2.6** in Figure 2.12, respectively, were used as a FRET pair because of overlap in emission and excitement in donor and acceptor. Compound **2.5** was synthesized via a coupling reaction that involved generation of a common boronic acid precursor appended to an amine functionality, which can be modified via specific reactions, such as reductive amination or coupling, to introduce different fluorophores, which entails modification in the final step. Another option would be to couple the amine to the fluorophore first, followed by addition of the boronic acid, as that would simplify the purification step. The two synthetic routes are shown in Figure 2.13 as 2.13A and 2.13B.

In addition, two different guests were involved in FRET studies, a catechol compound, **2.7** in Figure 2.12, (synthesized by Manpreet Kaur Cheema) and a mannose compound, **2.8** in Figure 2.12, (synthesized by Irene Abia). The idea of using divalent guests arose because we wanted to create a system that could imitate cell-surface carbohydrate clustering involving sugar molecules in the near vicinity. In order to activate FRET, the diol moieties on the mannose sugars or catechol derivatives were connected via a linker, as shown in Figure 2.11, to bind the donor and acceptor on the

same molecule bringing them into closer proximity. As reported in literature,[95] the binding affinities of boronic acids towards catechol are higher than that for the mannose sugar counterparts.

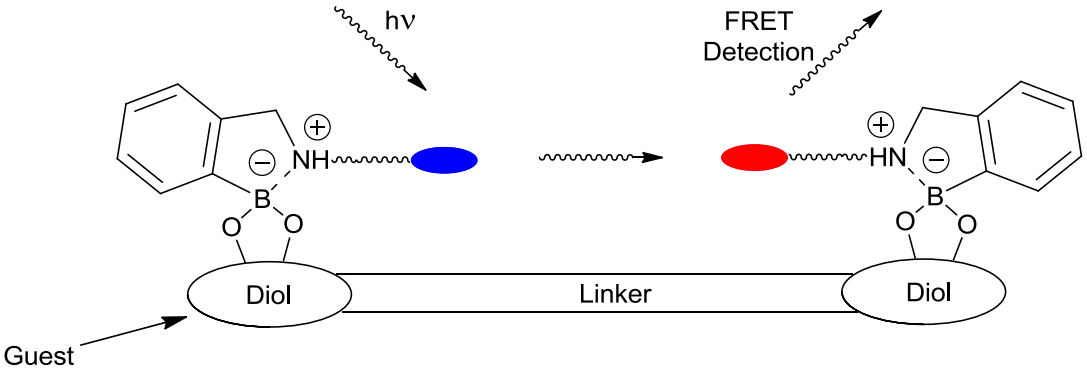

Figure 2.11. Schematic Representation of fluorophore-tagged boronic acids binding to guest

2.2.2 Research Synthesis

To synthesize the coumarin-tagged boronic acid, compund **2.5** as shown in Figure 2.7, two different synthetic routes were pursued as shown in Figure 2.13. The synthesis of coumarin-tagged boronic acid receptor **2.5** was initiated via mono-Boc protection of ethylenediamine. Afterwards, two different synthetic routes were attempted to observe which one was more efficient. The mono-Boc protected ethylenediamine was coupled with 2-formylphenylboronic acid via reductive amination to produce **2.2**. Boc deprotection of **2.2** using trifluoroacetic acid followed by EDC coupling gave compound **2.5**. This method provided us with an overall lower yield as purification of the polar compound **2.2** proved to be troublesome. Another option was for us to install the phenylboronic acid in the last step to make purification easier. The mono-Boc protected ethylenediamine was first coupled to coumarin-3-carboxylic acid to give compound **2.4** by EDC coupling. This was followed by Boc deprotection using trifluoroacetic acid and a substitution reaction with 2-bromomethylphenylboronic acid.

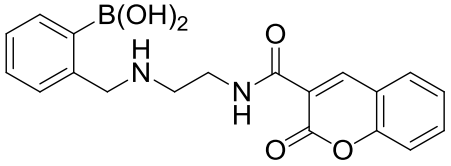

2.5

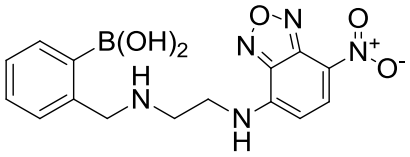

2.6 by Chí-Linh Đo-Thanh

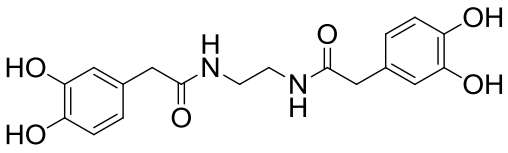

2.7 by Manpreet Kaur Chemma

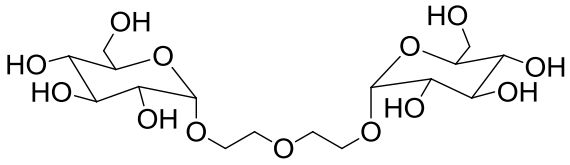

2.8 by Irene Abia

Figure 2.12. Target fluorophore tagged donor and acceptor and guests.

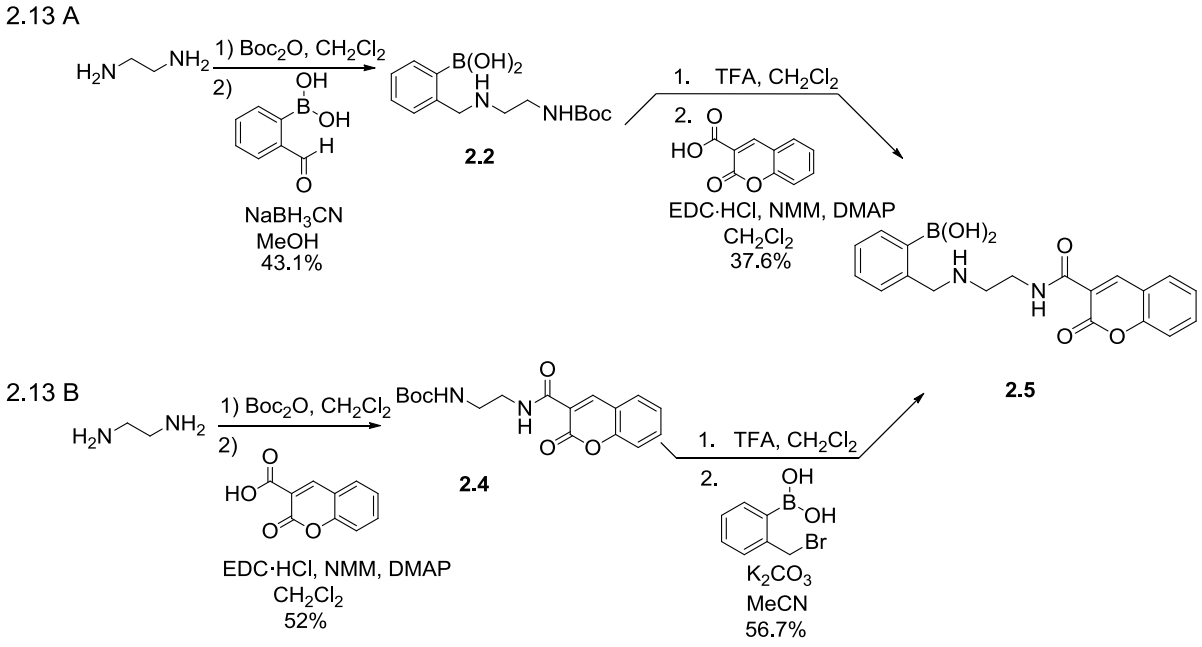

Figure 2.13. Synthesis of coumarin-tagged boronic acid receptor via routes 2.13A and 2.13 B.

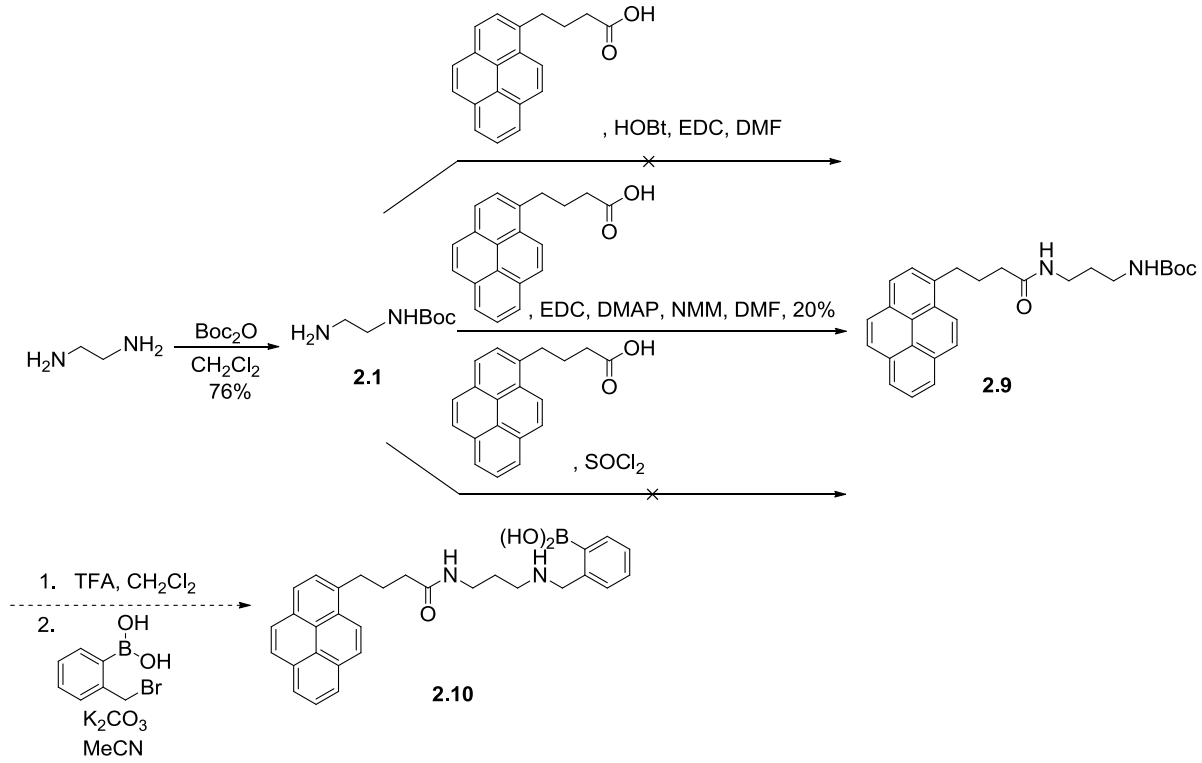

Figure 2.14. Synthesis of pyrene-tagged boronic acid receptor.

Attempts were made to synthesize pyrene-tagged boronic acid receptors for FRET detection as shown in Figure 2.14. Pyrene was selected for this purpose as it can function as both the donor and the acceptor. Unfortunately, the coupling of compound **2.1** to 1-pyrenebutyric acid to yield compound **2.9** proved to be problematic. 1-Ethyl-3-(3-dimethylaminopropyl)carbodiimide (EDC) coupling, when used with 4-dimethylaminopyridine (DMAP) and *N*-methylmorpholine (NMM), produces compound **2.9** but at a low yield of 20%. It is apparent that further optimization of reaction conditions is required.

2.2.3 Binding Studies

The fluorescence titration of coumarin and NBD-tagged boronic acid donor/ acceptor were meant to be completed with various diol-containing guests ranging from mannose- to catechol-based diol guests. During initial studies, the most promising results were obtained with HEPES buffer near neutral pH, and this was used for the binding titrations conducted.

Titrations were conducted using a fluorimeter to observe any fluctuations in fluorescence intensities of the donor and acceptor. We expect to see a gradual decrease in the coumarin emission signal and a gradual increase the emission intensity of the acceptor NBD molecules upon titration with guests. Compound **2.7** solutions prepared in HEPES buffer (5 mM at pH 7.4) were titrated against donor/acceptor solution (13.6 μM) and reasonable results were obtained as shown in Figure 2.15.

However, it was odd that the emission of NBD increased and then decreased. Thus, it is important that more work is done to optimize the conditions of FRET.

a)

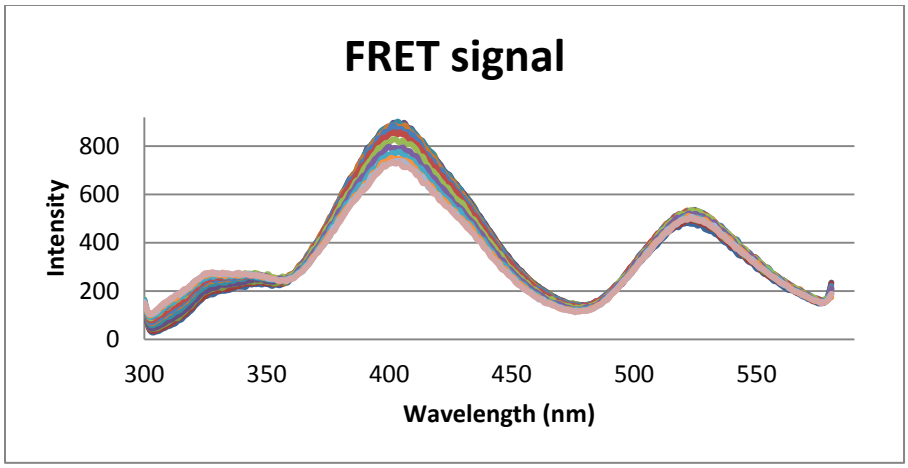

b)

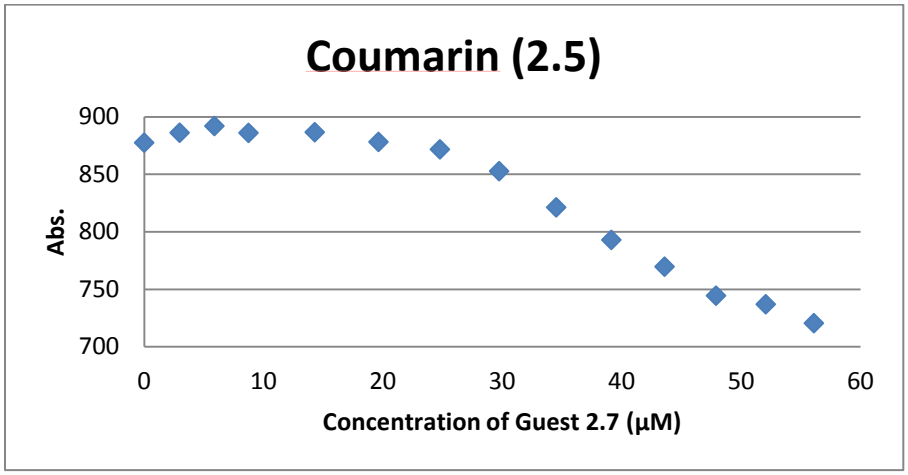

c)

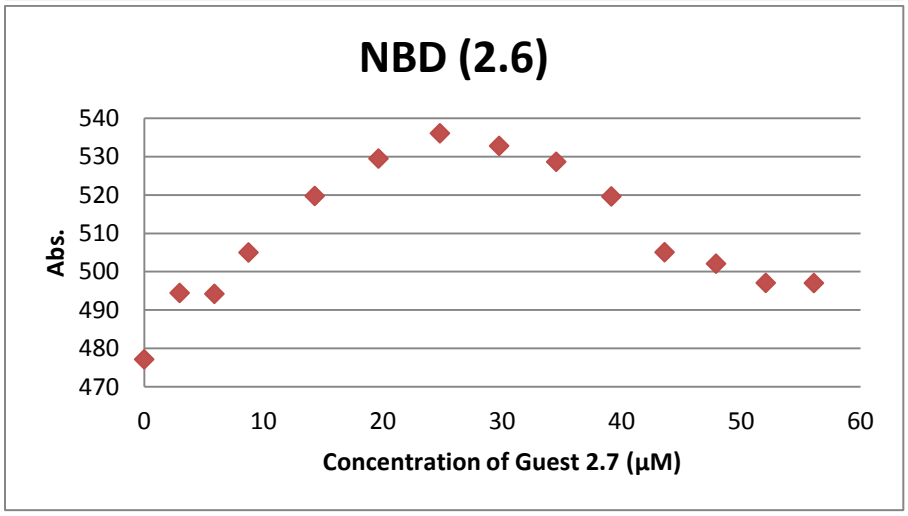

Figure 2.15 FRET-based fluorescence studies
a) FRET donor–acceptor signal
b) Decrease in fluorescence signal of Coumarin
c) Increase and then decrease in fluorescence signal of NBD

2.3 Experimental

Tert-Butyl (2-aminoethyl)carbamate (**2.1**)

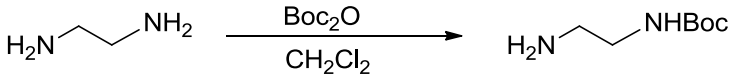

2.1

Ethane-1,2-diamine (12.0 mL, 179 mmol) was dissolved in dichloromethane (20 mL) and stirred. A solution of di-*tert*-butyldicarbonate (3.91 g, 17.9 mmol) in dichloromethane (40 mL) was then added dropwise via an addition funnel. The mixture was stirred overnight at room temperature and then extracted with dichloromethane (2 x 50 mL) from saturated aqueous sodium carbonate (50 mL). The combined organic layers were dried over magnesium sulfate, filtered and concentrated to give the product **2.1** (1.99 g, 76%) as a yellow oil. Characterization matched prior literature.[98]

^{1}H NMR (300 MHz, $CDCl_3$) δ 4.99 (s, 1H), 3.17 (q, *J* = 5.9 Hz, 2H), 2.80 (t, *J* = 6.4, 5.5 Hz, 2H), 1.45 (s, 9H) ppm.

(2-(((2-((*tert*-Butoxycarbonyl)amino)ethyl)amino)methyl)phenyl)boronic acid (**2.2**)

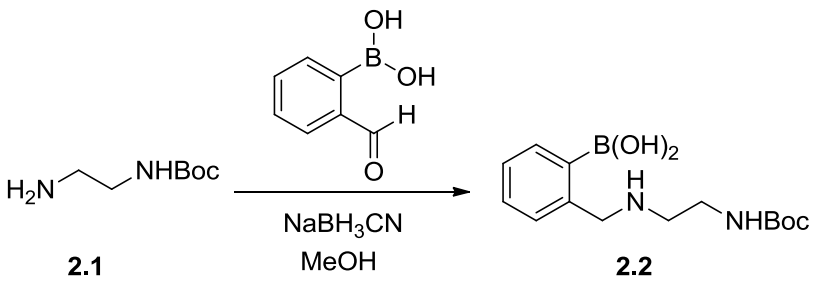

2.1 **2.2**

2.1 (0.312 g, 1.95 mmol) and 2-formylphenylboronic acid (0.327 g, 2.14 mmol) are added to round bottom flask and the flask was stoppered to have the air removed under vacuum. A nitrogen balloon was attached to the flask and the solution was stirred. Methanol (25 mL) was then added via a syringe and sodium cyanoborohydride (0.283 g, 4.28 mmol) was added in methanol via a syringe as well. The solution was then stirred overnight at room temperature, and then concentrated. Purification on a reversed-phase column (10 g, C18) with gradient elution from 0 to 100% methanol/water gave the product as a white solid **2.2** (0.247 g, 43%).

^{1}H NMR (300 MHz, CD_3OD) δ 7.45–7.39 (m, 1H), 7.24–7.11 (m, 3H), 4.05 (s, 2H), 3.39 (t, *J* = 6 Hz, 2H), 2.97 (t, *J* = 6 Hz, 2H), 1.44 (s, 9H).

2-((2-Boronobenzyl)amino)ethanaminium 2,2,2-trifluoroacetate (**2.3**)

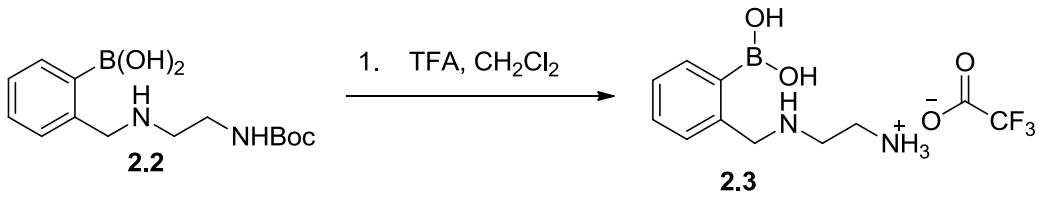

2.2 **2.3**

Trifluoroacetic acid (7 mL) was added to a solution of **2.2** (0.176 g, 0.597 mmol) in dichloromethane (7 mL). The reaction mixture was stirred in the dark at room temperature for 3 hours and then concentrated and dried under vacuum to obtain a yellow solid of trifluoroacetate salts (0.298 g, 162%). The high yield is due to the leftover trifluoroacetic acid and will be removed in the next step of the synthesis.

^{1}H NMR (300 MHz, CD_3OD) δ 7.77 (s, 1H), 7.44 (s, 3H), 4.34 (s, 2H), 3.38–3.33 (m, 4H) ppm.

tert-Butyl (2-(2H-chromene-3-carboxamido)ethyl)carbamate (**2.4**)

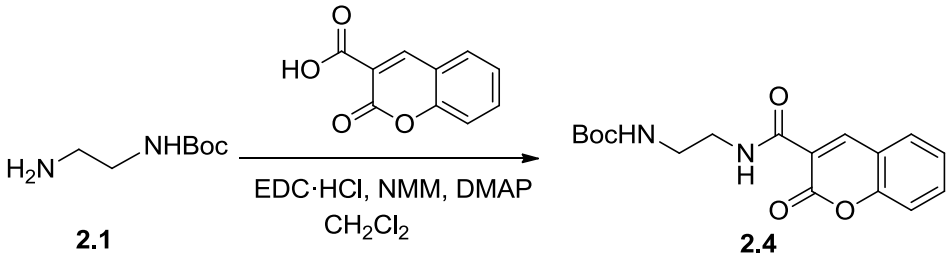

2.1 **2.4**

To a stirred solution of compound **2.1** (0.111 g, 0.705 mmol) in dichloromethane (8 mL) was added coumarin-3-carboxylic acid (0.1118 g, 0.588 mmol), *N*-methylmorpholine (129 µL, 1.18 mmol) and 4-dimethylaminopyridine (0.0718 g, 0.588 mmol). The solution was then cooled to 0 ^{o}C and stirred for 15 minutes. 1-Ethyl-3-(3-dimethylaminopropyl)carbodiimide in hydrochloride (0.135 g, 0.705 mmol) then added at 0 ^{o}C, and the reaction was stirred overnight while warming to room temperature. Afterwards, the solution was extracted with dichloromethane (12 mL) and water (20 mL). After collecting the organic layer, the aqueous layer was washed again with dichloromethane (20 mL). The organic layers were combined and dried with anhydrous magnesium sulfate, filtered, and the solvent was removed. Column chromatography with silica gel and a solvent gradient of 1%–5% methanol/ dichloromethane yielded **2.2** (0.124 g, 53%) as a yellow powder.

^{1}H NMR (300 MHz, $CDCl_3$) δ 9.00 (s, 1H), 8.90 (d, *J* = 0.7 Hz, 1H), 7.86–7.56 (m, 2H), 7.55–7.23 (m, 2H), 5.20 (s, 1H), 5.09 (s, 1H), 3.60 (q, *J* = 3.0 Hz, 2H), 3.40 (q, *J* = 6.0 Hz, 2H), 1.44 (s, 9H) ppm.

HRMS $[M+ H]_+$ calcd: 333.1372, found: 333.1342

2-(((2-(2-Oxo-*2H*-chromene-3-carboxamido)ethyl)amino)methyl)phenylboronic acid (**2.5**)

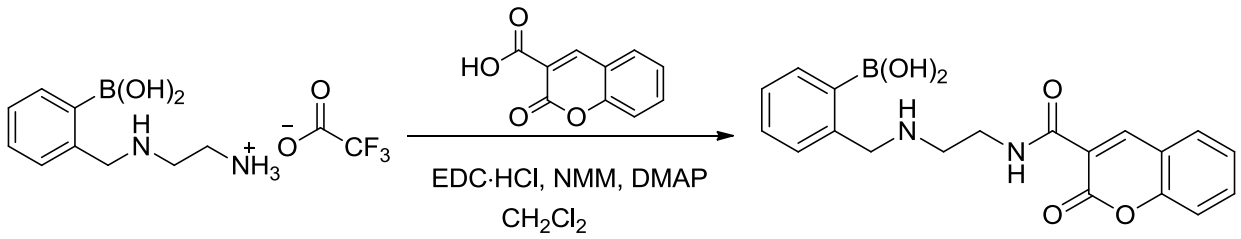

2.2 **2.5**

To a stirred solution of compound **2.2** (0.074 g, 0.214 mmol) in dichloromethane (5 mL) and acetonitrile (5 mL) was added coumarin-3-carboxylic acid (0.0338 g, 0.178 mmol), N-methylmorpholine (39.1 µL, 0.356 mmol) and 4-dimethylaminopyridine (0.0217 g, 0.178 mmol). The solution was then cooled to 0 ^{o}C and stirred for 15 minutes. 1-Ethyl-3-(3-dimethylaminopropyl)carbodiimide in hydrochloride (0.0410 g, 0.214 mmol) then added at 0 ^{o}C, and the reaction was stirred overnight while warming to room temperature. Afterwards, the solution was concentrated and then extracted with dichloromethane (20 mL) and water (20 mL). After collecting the organic layer, the aqueous layer was washed again with dichloromethane (20 mL). The organic layers were combined and dried with anhydrous magnesium sulfate, filtered, and the solvent was removed. Purification on a reversed-phase column (10 g, C18) with gradient elution from 0 to 100% methanol/water gave the product as a yellow solid **2.5** (0.245 g, 38 %).

^{1}H NMR (300 MHz, CD_3OD) δ 8.87 (s, 1H), 7.88–7.80 (m, 1H), 7.80-7.70 (m, 1H) 7.44 (m, 4H), 7.26 (s, 2H), 7.02 (s, 1H), 4.19 (d, *J* = 14.6 Hz, 2H), 3.81 (s, 2H), 3.25–3.07 (m, 2H).

tert-Butyl (2-(4-(pyren-1-yl)butanamido)ethyl)carbamate (**2.9**)

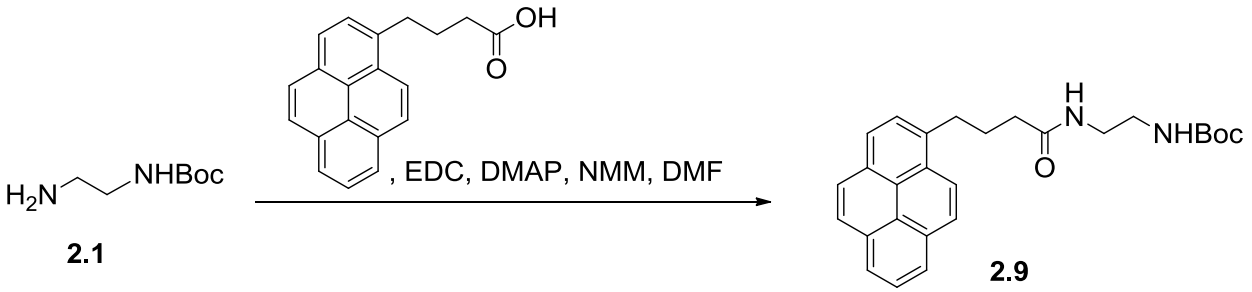

2.1 **2.9**

To a stirred solution of compound **2.1** (0.677 g, 4.23 mmol) in *N,N*– dimethylformamide (5 mL) was added 1-pyrenebutyric acid (0.813 g, 0.282 mmol), *N*-methylmorpholine (0.612 mL, 2.82 mmol) and 4-dimethylaminopyridine (0.344 g, 2.82 mmol). The solution was then cooled to 0 ^{o}C and stirred for 15 minutes. 1-Ethyl-3-(3 dimethylaminopropyl)carbodiimide in hydrochloride (0.811 g, 4.23 mmol) was then added at 0 ^{o}C, and the reaction was stirred overnight while warming to room temperature. Afterwards, the solution was concentrated and then extracted with dichloromethane (20 mL) and water (20 mL). After collecting the organic layer, the aqueous layer was washed again with dichloromethane (20 mL) twice. The organic layers were combined and dried with anhydrous magnesium sulfate, filtered, and the solvent was removed. Column chromatography with silica gel and a solvent gradient of 40%–60% ethyl acetate/ hexane yielded **2.9** (0.243 g, 20%) as a yellow powder.

^{1}H NMR (300 MHz, $CDCl_3$) δ 8.38–8.32 (m, 1H), 8.20–8.08 (m, 4H), 8.04–8.01 (m, 2H), 7.99 (d, *J* = 2.1 Hz, 1H), 7.87 (dd, *J* = 7.8, 3.7 Hz, 1H), 3.58 (p, *J* = 6 Hz, 2H), 3.45 (d, *J* = 7.7 Hz, 2H), 2.44–2.32 (m, 2H), 2.32 – 2.16 (m, 2H), 1.62 (s, 2H), 1.47 (s, 9H).

Chapter 3 Miscellaneous Microarray Analysis and Synthetic Compounds

3.1 Synthesis of *N*-(4-nitrobenzenesulfonyl) alanine and *N*-(4-nitrophenyl) alanine

For a collaborative project with Dr. Robert Compton, we synthesized *N*-(4-nitrobenzenesulfonyl)-L-alanine (3.2a), *N*-(4-nitrobenzenesulfonyl)-D-alanine (3.2b), *N*-(4-nitrophenyl)-L-alanine (3.3a) and *N*-(4-nitrophenyl)-D-alanine (3.3b) to study their circular dichroism (CD) and negative-ion properties.

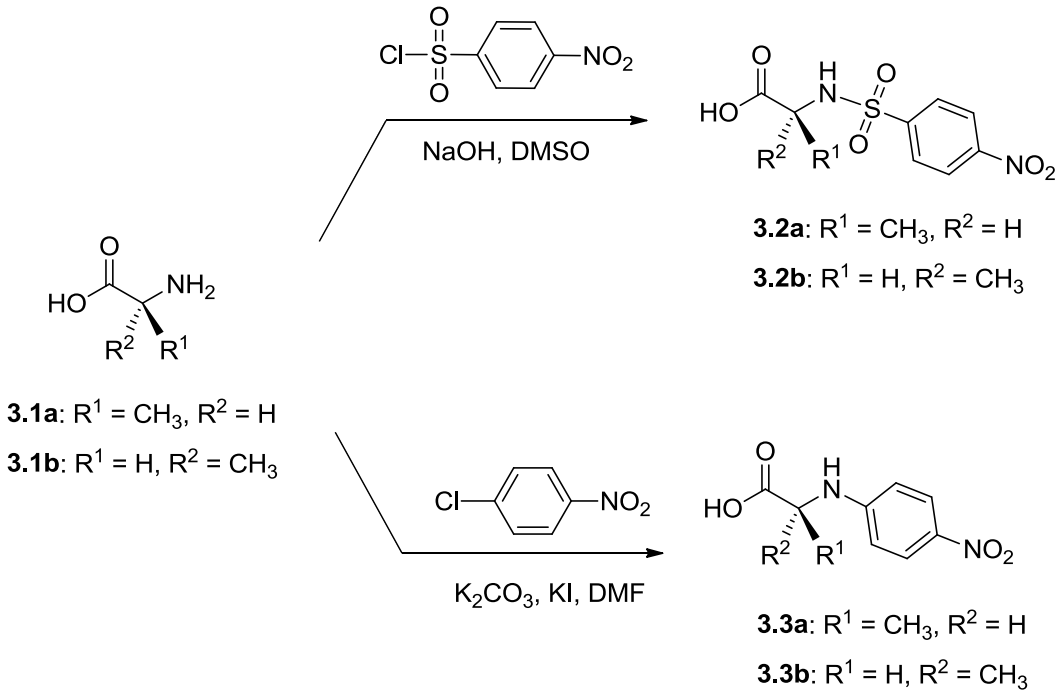

Figure 3.1. Synthesis of alanine analogues

Experimental

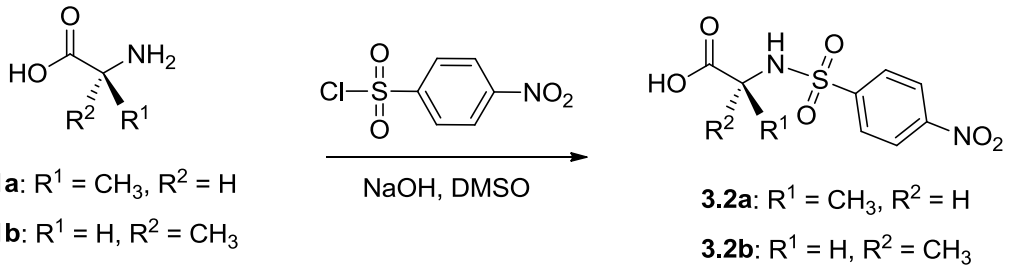

3.1a: $R^1 = CH_3$, $R^2 = H$

3.1b: $R^1 = H$, $R^2 = CH_3$

3.2a: $R^1 = CH_3$, $R^2 = H$

3.2b: $R^1 = H$, $R^2 = CH_3$

N-(4-nitrobenzenesulfonyl)-L-alanine (3.2a) and *N*-(4-nitrobenzenesulfonyl)-D-alanine (3.2b) To produce compound 3.2a, an aqueous 1 M sodium hydroxide solution (5 mL) was added to L-alanine (3.2a, 1.00 g, 11.3 mmol), followed by cooling to 0 °C. 4-Nitrobenzenesulfonyl chloride (3.82 g, 16.9 mmol) was next added in small portions, and the reaction mixture was stirred at rt overnight, followed by washing with ethyl acetate (2 × 10 mL). The aqueous layer was then acidified with 1 M hydrochloric acid (10 mL) and extracted with ethyl acetate (15 mL). The latter organic layer was dried with magnesium sulfate, filtered, and concentrated. Column chromatography over silica gel with gradient elution from 5 to 20% methanol/dichloromethane gave the product as a yellow solid (0.71 g, 31%). Enantiomer 3.2b was similarly prepared using D-alanine (3.1b, 1.01 g, 11.3 mmol), 1 M sodium hydroxide (7 mL) and 4-nitrobenzenesulfonyl chloride (3.82 g, 16.9 mmol), which yielded 3.2b as a light yellow solid (0.831 g, 35%).

^{1}H NMR (300 MHz, DMSO-d_6) δ 8.37 (d, *J* = 7.1 Hz, 2H), 8.04 (d, *J* = 7.1 Hz, 2H), 3.68 (q, *J* = 7.1 Hz, 1H), 1.19 (d, *J* = 7.1 Hz, 3H).

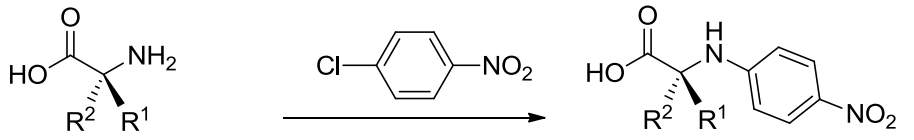

3.1a: $R^1 = CH_3$, $R^2 = H$

3.1b: $R^1 = H$, $R^2 = CH_3$

3.3a: $R^1 = CH_3$, $R^2 = H$

3.3b: $R^1 = H$, $R^2 = CH_3$

N-(4-nitrophenyl)-L-alanine (3a) and *N*-(4-nitrophenyl)-D-alanine (3b) To produce compound 3a, 20 mL of *N,N*-dimethylformamide (DMF) was added to L-alanine (1a, 0.950 g, 10.7 mmol). Potassium carbonate (2.95 g, 21.3 mmol) and potassium iodide (1.77 g, 10.7 mmol) were then added to the stirring solution. 4-Chloronitrobenzene (3.36 g, 21.3 mmol) was next added in small portions, and the reaction mixture was stirred and refluxed at 120 ^{o}C overnight. Next, the solvent was removed via rotary evaporation. The crude product was then dissolved in 50 mL of water, acidified with 1 M hydrochloric acid (20 mL), and extracted with ethyl acetate (2 x 25 mL). The latter organic layer was dried with magnesium sulfate, filtered, and concentrated. Column chromatography over silica gel with gradient elution from 1 to 25% methanol/dichloromethane gave the product as a yellow solid (1.21 g, 54%). Enantiomer 3b was similarly prepared using D-alanine (1b, 0.880 g, 9.90 mmol), 20 mL of DMF, potassium carbonate (2.74 g, 19.8 mmol), tetrabutylammonium iodide (3.66 g, 9.90 mmol) and 4-chloronitrobenzene (3.12g, 19.8 mmol), which yielded 3b as a yellow solid (0.67 g, 32%). ^{1}H NMR (300 MHz, Methanol- d_4) δ 8.02 (d, J = 9 Hz, 2H), 6.60 (d, J = 9 Hz, 2H), 3.96 (q, J = 9 Hz, 1H), 1.48 (d, J=9 Hz, 3H, –CH_3).

3.2 Carbohydrate Microarray Analysis

For a collaborative project with Dr. David Baker, we will utilize covalent immobilization of thiol-terminated sugars as shown in Figure 3.2 onto epoxide functionalized slides. This allows for a very stable glycan microarray for interrogation with proteins. This project was previously worked on by Irene Abia from the Baker lab.

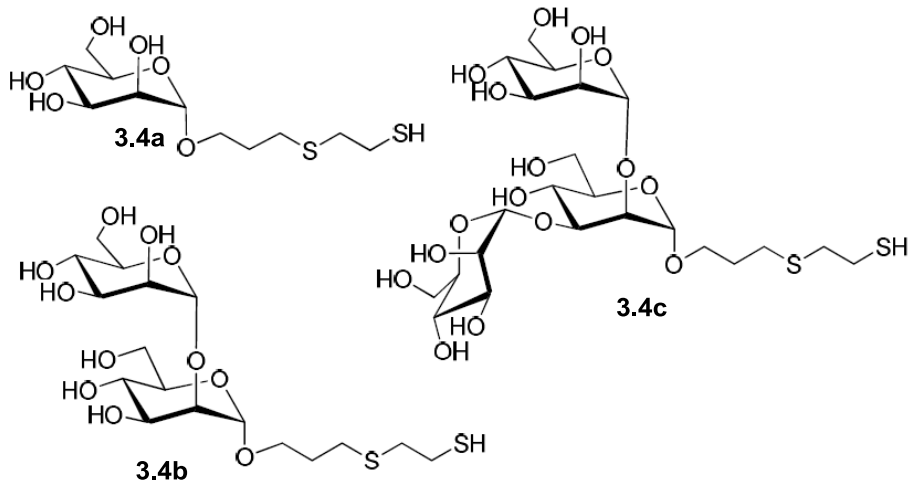

Figure 3.2. Thiol-terminated mannose used in binding studies.

Using robotic printing technology, thiol-terminated mannose derivatives **3.4a, 3.4b** and **3.4c** were printed onto epoxide-functionalized glass slides (Figure 3.2) to achieve covalent immobilization.

3.2.1 Experimental

3.2.1.1 Materials

Epoxide-derivatized glass slides (Nexterion slide E, SCHOTT North America), Rhodamine labeled Conconavalin A (Vector Labs), thiol-terminated mannose derivatives; all other standard chemicals were purchased from commercial suppliers and used as received. Glass slides were stored in a desiccator to keep them dry.

3.2.1.2. Methods

Printing sugar solutions were made up of sugar, PBS (30 mM phosphate-buffered saline and 0.05% Tween-20) of pH 8.5 and TCEP. The final TCEP concentration in each prepared sugar solution was 2 mM. On a single glass slide, 12 different concentrations (0, 25, 50,100, 150, 200, 250, 300, 400, 500, 750, 1000 μM) of each sugar were probed with 6 different concentrations of protein Con A (0, 5, 10, 20, 30, 50 μg/mL, which corresponds to 0, 48, 96, 192, 288 and 481 nM, respectively). Using the standard robotic pin printer (Virtek ChipwriterTM Professional Arrayer, Figure 20), the different solutions of sugars were printed on epoxide functionalized glass slides. Each super grid had 3 grids, and each grid was printed in a 12 × 10 pattern. After an overnight incubation at room temperature, slides were washed by submerging them in Petri dishes filled with wash buffer (PBS, pH 7.4 containing 0.05% Tween-20) and gently shaking on a waver for 30 min. To block unreacted epoxides, slides were submerged in Petri dishes filled with a block solution (50 mM ethanolamine in 100 mM borate, pH 9.2) and gently shaken for 1 h on a waver. After blocking, the slides were washed three times by immersing them in Petri dishes filled with PBS buffer (pH 8.4)

and dried by gentle purging with N_2 air. Slides were immediately used for incubation with protein.

Rhodamine-labeled Con A (5 mg/mL) was diluted in PBS buffer. Six different concentrations of Con A were obtained: 2, 5, 10, 20, 30 and 50 µg/mL. An incubation chamber was fabricated by placing a damp, warm paper towel in a covered plastic box. The IC-16 chamber from Nexterion was used to separate the supergrids. For incubations, 120 µL of protein solution was applied to each supergrid, and slides were placed in the incubation chamber and placed on the shaker for 1 h at room temperature. After incubation, slides were washed three times in Petri dishes filled with wash buffer for three times with distilled water, and then dried by gentle purging with N_2 air to ensure complete dryness. Each wash was approximately 5 min. The dried plates were scanned immediately to obtain results.

3.2.2 Preliminary Results

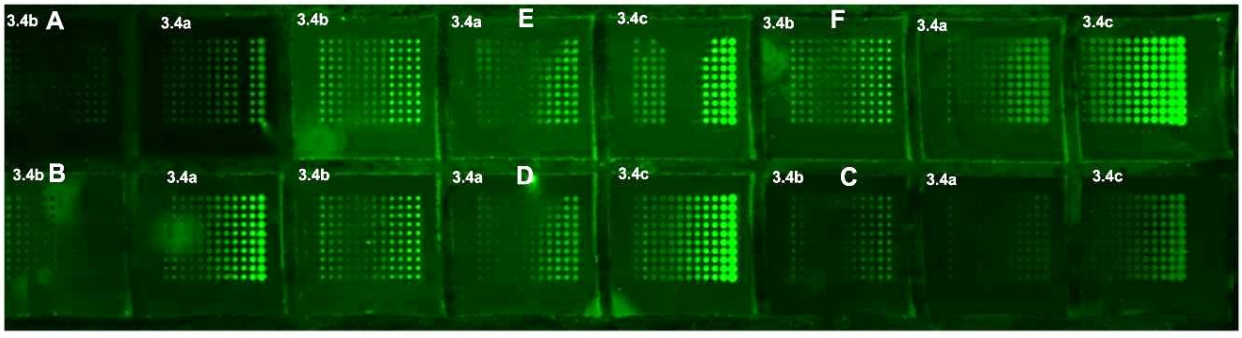

Figure 3.3. Scanned image of glycan microarray with Con A. Monosaccharide 3.4a, disaccharide 3.4b, and trisaccharide 3.4c. Protein concentrations: 0 µg/mL (A), 5µg/mL (B), 10 µg/mL (C), 20 µg/mL (D), 30 µg/mL (E) and 50 µg/mL (F).

Preliminary results of microarray analysis proved to be successful as increasing fluorescence intensity is observed with increasing protein concentration and glycan concentration. Interestingly, the grids incubated with no protein concentration showed fluorescence and that should not have been the case. However, work remains to be done as this assay requires that perfectly printed supergrids and the slide shown in Figure 3.3 has a few grids which were not completed printed. It is necessary that we improve on and optimize the current conditions.

List of References

1. Lindhorst, T. K., *Essentials of Carbohydrate Chemistry and Biochemistry*. 3rd ed.; Wiley-VCH: 2007; p 332.
2. Garett, R. G., C.M., *Biochemistry*. 3rd ed.; Thomson Brook/ Cole: Belmont, CA, 2005.
3. Dube, D. H.; Bertozzi, C. R., Glycans in cancer and inflammation--potential for therapeutics and diagnostics. *Nat Rev Drug Discov* **2005,** *4* (6), 477-88.
4. Focarelli, R.; La Sala, G. B.; Balasini, M.; Rosati, F., Carbohydrate-mediated sperm-egg interaction and species specificity: a clue from the Unio elongatulus model. *Cells Tissues Organs* **2001,** *168* (1-2), 76-81.
5. Rosati, F.; Capone, A.; Giovampaola, C. D.; Brettoni, C.; Focarelli, R., Sperm-egg interaction at fertilization: glycans as recognition signals. *Int J Dev Biol* **2000,** *44* (6), 609-18.
6. Goodman, J. L.; Nelson, C. M.; Klein, M. B.; Hayes, S. F.; Weston, B. W., Leukocyte infection by the granulocytic ehrlichiosis agent is linked to expression of a selectin ligand. *J. Clin. Invest.* **1999,** *103* (3), 407-12.
7. Bicker, K. L.; Sun, J.; Lavigne, J. J.; Thompson, P. R., Boronic acid functionalized peptidyl synthetic lectins: combinatorial library design, peptide sequencing, and selective glycoprotein recognition. *ACS Comb Sci* **2011,** *13* (3), 232-43.
8. Meezan, E.; Wu, H. C.; Black, P. H.; Robbins, P. W., Comparative studies on the carbohydrate-containing membrane components of normal and virus-transformed mouse fibroblasts. II. Separation of glycoproteins and glycopeptides by sephadex chromatography. *Biochemistry* **1969,** *8* (6), 2518-24.
9. Hakomori, S., Aberrant glycosylation in cancer cell membranes as focused on glycolipids: overview and perspectives. *Cancer Res.* **1985,** *45* (6), 2405-14.
10. Sell, S., Cancer-associated carbohydrates identified by monoclonal antibodies. *Hum Pathol* **1990,** *21* (10), 1003-19.
11. Adachi, M.; Hayami, M.; Kashiwagi, N.; Mizuta, T.; Ohta, Y.; Gill, M. J.; Matheson, D. S.; Tamaoki, T.; Shiozawa, C.; Hakomori, S., Expression of Ley antigen in human immunodeficiency virus-infected human T cell lines and in peripheral lymphocytes of patients with acquired immune deficiency syndrome (AIDS) and AIDS-related complex (ARC). *J. Exp. Med.* **1988,** *167* (2), 323-31.
12. Nakaishi, H.; Sanai, Y.; Shibuya, M.; Iwamori, M.; Nagai, Y., Neosynthesis of neolacto- and novel ganglio-series gangliosides in a rat fibroblastic cell line brought about by transfection with the v-fes oncogene-containing Gardner-Arnstein strain feline sarcoma virus-DNA. *Cancer Res.* **1988,** *48* (7), 1753-8.
13. Schachter, H.; Jaeken, J., Carbohydrate-deficient glycoprotein syndrome type II. *Biochim. Biophys. Acta* **1999,** *1455* (2-3), 179-92.
14. Hollingsworth, M. A.; Swanson, B. J., Mucins in cancer: protection and control of the cell surface. *Nat. Rev. Cancer* **2004,** *4* (1), 45-60.
15. (a) Hakomori, S.; Zhang, Y., Glycosphingolipid antigens and cancer therapy. *Chem. Biol.* **1997,** *4* (2), 97-104; (b) Hakomori, S., Traveling for the glycosphingolipid path. *Glycoconj J* **2000,** *17* (7-9), 627-47.

16. Zhang, S.; Cordon-Cardo, C.; Zhang, H. S.; Reuter, V. E.; Adluri, S.; Hamilton, W. B.; Lloyd, K. O.; Livingston, P. O., Selection of tumor antigens as targets for immune attack using immunohistochemistry: I. Focus on gangliosides. *Int. J. Cancer* **1997,** *73* (1), 42-9.
17. Fukuda, M., Possible roles of tumor-associated carbohydrate antigens. *Cancer Res.* **1996,** *56* (10), 2237-44.
18. Zhang, J.; Nakayama, J.; Ohyama, C.; Suzuki, M.; Suzuki, A.; Fukuda, M.; Fukuda, M. N., Sialyl Lewis X-dependent lung colonization of B16 melanoma cells through a selectin-like endothelial receptor distinct from E- or P-selectin. *Cancer Res.* **2002,** *62* (15), 4194-8.
19. Gout, S.; Tremblay, P. L.; Huot, J., Selectins and selectin ligands in extravasation of cancer cells and organ selectivity of metastasis. *Clin Exp Metastasis* **2008,** *25* (4), 335-44.
20. Ben-David, T.; Sagi-Assif, O.; Meshel, T.; Lifshitz, V.; Yron, I.; Witz, I. P., The involvement of the sLe-a selectin ligand in the extravasation of human colorectal carcinoma cells. *Immunol. Lett.* **2008,** *116* (2), 218-24.
21. Kobayashi, H.; Boelte, K. C.; Lin, P. C., Endothelial cell adhesion molecules and cancer progression. *Curr. Med. Chem.* **2007,** *14* (4), 377-86.
22. Kannagi, R., Carbohydrate antigen sialyl Lewis a--its pathophysiological significance and induction mechanism in cancer progression. *Chang Gung Med J* **2007,** *30* (3), 189-209.
23. Hakomori, S., Tumor-associated carbohydrate antigens defining tumor malignancy: basis for development of anti-cancer vaccines. *Adv. Exp. Med. Biol.* **2001,** *491*, 369-402.
24. Kim, Y. J.; Varki, A., Perspectives on the significance of altered glycosylation of glycoproteins in cancer. *Glycoconj J* **1997,** *14* (5), 569-76.
25. Gabius, H. J., Biological and clinical implications of tumor lectins: present status and future prospects. *Acta Histochem Suppl* **1988,** *36*, 209-16.
26. Orntoft, T. F.; Vestergaard, E. M., Clinical aspects of altered glycosylation of glycoproteins in cancer. *Electrophoresis* **1999,** *20* (2), 362-71.
27. (a) Gold, P.; Freedman, S. O., Demonstration of Tumor-Specific Antigens in Human Colonic Carcinomata by Immunological Tolerance and Absorption Techniques. *J. Exp. Med.* **1965,** *121*, 439-62; (b) Gold, P.; Freedman, S. O., Specific carcinoembryonic antigens of the human digestive system. *J. Exp. Med.* **1965,** *122* (3), 467-81.
28. Thomas, P.; Toth, C. A.; Saini, K. S.; Jessup, J. M.; Steele, G., Jr., The structure, metabolism and function of the carcinoembryonic antigen gene family. *Biochim. Biophys. Acta* **1990,** *1032* (2-3), 177-89.
29. Macdonald, J. S., Carcinoembryonic antigen screening: pros and cons. *Semin Oncol* **1999,** *26* (5), 556-60.
30. Patankar, M. S.; Jing, Y.; Morrison, J. C.; Belisle, J. A.; Lattanzio, F. A.; Deng, Y.; Wong, N. K.; Morris, H. R.; Dell, A.; Clark, G. F., Potent suppression of natural killer cell response mediated by the ovarian tumor marker CA125. *Gynecol Oncol* **2005,** *99* (3), 704-13.

31. (a) Basu, P. S.; Majhi, R.; Batabyal, S. K., Lectin and serum-PSA interaction as a screening test for prostate cancer. *Clin. Biochem.* **2003,** *36* (5), 373-6; (b) Peracaula, R.; Tabares, G.; Royle, L.; Harvey, D. J.; Dwek, R. A.; Rudd, P. M.; de Llorens, R., Altered glycosylation pattern allows the distinction between prostate-specific antigen (PSA) from normal and tumor origins. *Glycobiology* **2003,** *13* (6), 457-70.
32. Zou, Y.; Broughton, D. L.; Bicker, K. L.; Thompson, P. R.; Lavigne, J. J., Peptide borono lectins (PBLs): a new tool for glycomics and cancer diagnostics. *ChemBioChem* **2007,** *8* (17), 2048-51.
33. Taylorpapadimitriou, J.; Gendler, S., Structure, biology and possible clinical-applications of carcinoma-associated mucins. *Int J Oncol* **1992,** *1* (1), 9-16.
34. (a) Burchell, J. M.; Mungul, A.; Taylor-Papadimitriou, J., O-linked glycosylation in the mammary gland: changes that occur during malignancy. *J Mammary Gland Biol Neoplasia* **2001,** *6* (3), 355-64; (b) Lloyd, K. O.; Burchell, J.; Kudryashov, V.; Yin, B. W.; Taylor-Papadimitriou, J., Comparison of O-linked carbohydrate chains in MUC-1 mucin from normal breast epithelial cell lines and breast carcinoma cell lines. Demonstration of simpler and fewer glycan chains in tumor cells. *J. Biol. Chem.* **1996,** *271* (52), 33325-34.
35. (a) Taylor-Papadimitriou, J.; Epenetos, A. A., Exploiting altered glycosylation patterns in cancer: progress and challenges in diagnosis and therapy. *Trends Biotechnol.* **1994,** *12* (6), 227-33; (b) Sivolapenko, G. B.; Douli, V.; Pectasides, D.; Skarlos, D.; Sirmalis, G.; Hussain, R.; Cook, J.; Courtenay-Luck, N. S.; Merkouri, E.; Konstantinides, K.; et al., Breast cancer imaging with radiolabelled peptide from complementarity-determining region of antitumour antibody. *Lancet* **1995,** *346* (8991-8992), 1662-6.
36. Moore, A.; Medarova, Z.; Potthast, A.; Dai, G., In vivo targeting of underglycosylated MUC-1 tumor antigen using a multimodal imaging probe. *Cancer Res.* **2004,** *64* (5), 1821-7.
37. Yan, J.; Fang, H.; Wang, B., Boronolectins and fluorescent boronolectins: an examination of the detailed chemistry issues important for the design. *Med. Res. Rev.* **2005,** *25* (5), 490-520.
38. Gunnarsson, L. C.; Dexlin, L.; Karlsson, E. N.; Holst, O.; Ohlin, M., Evolution of a carbohydrate binding module into a protein-specific binder. *Biomol. Eng.* **2006,** *23* (2-3), 111-7.
39. Turner, G. A., N-glycosylation of serum proteins in disease and its investigation using lectins. *Clin. Chim. Acta* **1992,** *208* (3), 149-71.
40. Lin, N.; Yan, J.; Huang, Z.; Altier, C.; Li, M.; Carrasco, N.; Suyemoto, M.; Johnston, L.; Wang, S.; Wang, Q.; Fang, H.; Caton-Williams, J.; Wang, B., Design and synthesis of boronic-acid-labeled thymidine triphosphate for incorporation into DNA. *Nucleic Acids Res.* **2007,** *35* (4), 1222-9.
41. Adhikari, P.; Bachhawat-Sikder, K.; Thomas, C. J.; Ravishankar, R.; Jeyaprakash, A. A.; Sharma, V.; Vijayan, M.; Surolia, A., Mutational analysis at Asn-41 in peanut agglutinin. A residue critical for the binding of the tumor-associated Thomsen-Friedenreich antigen. *J. Biol. Chem.* **2001,** *276* (44), 40734-9.
42. Jin, S.; Cheng, Y.; Reid, S.; Li, M.; Wang, B., Carbohydrate recognition by boronolectins, small molecules, and lectins. *Med. Res. Rev.* **2010,** *30* (2), 171-257.

43. Michaelis, A. B., P., Ueber Monophenylborchlorid und die valenz des bors. *Ber. Dtsch. Chem. Ges.* **1880,** *13* (1), 58.
44. Sugihara JM, B. C., Cyclic benzeneboronate esters. *J. Am. Chem. Soc.* **1958,** *80*, 2443-2446.
45. J., B., The use of boric acid for the determination of the configuration of carbohydrates. *Adv Carbohydr Chem* **1949,** *4*, 189-210.
46. Kuivila, H. G., Keough, A. H., Soboczenski, E. J., Areneboronates from diols and polyols. *J. Org. Chem.* **1954,** *19* (5), 780-783.
47. Lorand JP, E. J., Polyol complexes and structure of the benzeneboronate ion. *J. Org. Chem.* **1959,** *24*, 769-774.
48. (a) Takeuchi, M.; Shinkai, S., [Saccharide sensing using a boronic-acid probe]. *Tanpakushitsu Kakusan Koso* **1996,** *41* (16), 2584-92; (b) Wang, W.; Gao, S.; Wang, B., Building fluorescent sensors by template polymerization: the preparation of a fluorescent sensor for D-fructose. *Org. Lett.* **1999,** *1* (8), 1209-12; (c) Yang, W.; He, H.; Drueckhammer, D. G., Computer-Guided Design in Molecular Recognition: Design and Synthesis of a Glucopyranose Receptor This work was supported by the National Institutes of Health (grant DK5523402). *Angew. Chem. Int. Ed. Engl.* **2001,** *40* (9), 1714-1718; (d) Draffin, S. P.; Duggan, P. J.; Duggan, S. A., Highly fructose selective transport promoted by boronic acids based on a pentaerythritol core. *Org. Lett.* **2001,** *3* (6), 917-20; (e) Edwards, N. Y.; Sager, T. W.; McDevitt, J. T.; Anslyn, E. V., Boronic acid based peptidic receptors for pattern-based saccharide sensing in neutral aqueous media, an application in real-life samples. *J. Am. Chem. Soc.* **2007,** *129* (44), 13575-83; (f) Sorensen, M. D.; Martins, R.; Hindsgaul, O., Assessing the terminal glycosylation of a glycoprotein by the naked eye. *Angew. Chem. Int. Ed. Engl.* **2007,** *46* (14), 2403-7.
49. (a) Burgemeister, T.; Grobeeinsler, R.; Grotstollen, R.; Mannschreck, A.; Wulff, G., ON THE CHEMISTRY OF BINDING-SITES .1. FAST THERMAL BREAKING AND FORMATION OF A B-N BOND IN 2-(AMINOMETHYL)BENZENEBORONATES. *Chem Ber-Recl* **1981,** *114* (10), 3403-3411; (b) Wulff, G.; Lauer, M.; Bohnke, H., ON THE CHEMISTRY OF BINDING-SITES .5. RAPID PROTON-TRANSFER AS CAUSE OF AN UNUSUALLY LARGE NEIGHBORING GROUP EFFECT. *Angew Chem Int Edit* **1984,** *23* (9), 741-742.
50. James, T. D.; Sandanayake, K.; Iguchi, R.; Shinkai, S., NOVEL SACCHARIDE-PHOTOINDUCED ELECTRON-TRANSFER SENSORS BASED ON THE INTERACTION OF BORONIC ACID AND AMINE. *J. Am. Chem. Soc.* **1995,** *117* (35), 8982-8987.
51. (a) Franzen, S.; Ni, W. J.; Wang, B. H., Study of the mechanism of electron-transfer quenching by boron-nitrogen adducts in fluorescent sensors. *J. Phys. Chem. B* **2003,** *107* (47), 12942-12948; (b) Ni, W.; Kaur, G.; Springsteen, G.; Wang, B.; Franzen, S., Regulating the fluorescence intensity of an anthracene boronic acid system: a B-N bond or a hydrolysis mechanism? *Bioorg. Chem.* **2004,** *32* (6), 571-81.
52. Zhu, L.; Shabbir, S. H.; Gray, M.; Lynch, V. M.; Sorey, S.; Anslyn, E. V., A structural investigation of the N-B interaction in an o-(N,N-dialkylaminomethyl)arylboronate system. *J. Am. Chem. Soc.* **2006,** *128* (4), 1222-32.

53. Wulff, G., SELECTIVE BINDING TO POLYMERS VIA COVALENT BONDS - THE CONSTRUCTION OF CHIRAL CAVITIES AS SPECIFIC RECEPTOR-SITES. *Pure Appl. Chem.* **1982,** *54* (11), 2093-2102.
54. Wiskur, S. L.; Lavigne, J. J.; Ait-Haddou, H.; Lynch, V.; Chiu, Y. H.; Canary, J. W.; Anslyn, E. V., pK(a) values and geometries of secondary and tertiary amines complexed to boronic acids - Implications for sensor design. *Org. Lett.* **2001,** *3* (9), 1311-1314.
55. (a) Cordes, D. B.; Miller, A.; Gamsey, S.; Sharrett, Z.; Thoniyot, P.; Wessling, R.; Singaram, B., Optical glucose detection across the visible spectrum using anionic fluorescent dyes and a viologen quencher in a two-component saccharide sensing system. *Org. Biomol. Chem.* **2005,** *3* (9), 1708-13; (b) Gamsey, S.; Miller, A.; Olmstead, M. M.; Beavers, C. M.; Hirayama, L. C.; Pradhan, S.; Wessling, R. A.; Singaram, B., Boronic acid-based bipyridinium salts as tunable receptors for monosaccharides and alpha-hydroxycarboxylates. *J. Am. Chem. Soc.* **2007,** *129* (5), 1278-86.
56. Billingsley, K.; Balaconis, M. K.; Dubach, J. M.; Zhang, N.; Lim, E.; Francis, K. P.; Clark, H. A., Fluorescent Nano-Optodes for Glucose Detection. *Anal. Chem.* **2010,** *82* (9), 3707-3713.
57. Springsteen, G.; Wang, B., Alizarin Red S. as a general optical reporter for studying the binding of boronic acids with carbohydrates. *Chem Commun (Camb)* **2001,** (17), 1608-9.
58. Niemeyer, C. M.; Ceyhan, B., DNA-Directed Functionalization of Colloidal Gold with Proteins This work was supported by Deutsche Forschungsgemeinschaft and Fonds der Chemischen Industrie. We thank Prof. D. Blohm for helpful discussions and generous support. *Angew. Chem. Int. Ed. Engl.* **2001,** *40* (19), 3685-3688.
59. Cannizzo, C.; Amigoni-Gerbier, S.; Larpent, C., Boronic acid-functionalized nanoparticles: synthesis by microemulsion polymerization and application as a re-usable optical nanosensor for carbohydrates. *Polymer* **2005,** *46* (4), 1269-1276.
60. Macbeath, G. K. A. N. S. S. L., Printing small molecules as microarrays and detecting protein- ligand interactions en masse *J. Am. Chem. Soc.* **1999,** *121* (34), 7967-7968.
61. MacBeath, G.; Schreiber, S. L., Printing proteins as microarrays for high-throughput function determination. *Science* **2000,** *289* (5485), 1760-3.
62. Fang, Y.; Frutos, A. G.; Lahiri, J., Membrane protein microarrays. *J. Am. Chem. Soc.* **2002,** *124* (11), 2394-5.
63. Ko, K. S.; Jaipuri, F. A.; Pohl, N. L., Fluorous-based carbohydrate microarrays. *J. Am. Chem. Soc.* **2005,** *127* (38), 13162-3.
64. Shin, I.; Cho, J. W.; Boo, D. W., Carbohydrate arrays for functional studies of carbohydrates. *Comb Chem High Throughput Screen* **2004,** *7* (6), 565-74.
65. Min, D. H.; Su, J.; Mrksich, M., Profiling kinase activities by using a peptide chip and mass spectrometry. *Angew. Chem. Int. Ed. Engl.* **2004,** *43* (44), 5973-7.
66. Kononen, J.; Bubendorf, L.; Kallioniemi, A.; Barlund, M.; Schraml, P.; Leighton, S.; Torhorst, J.; Mihatsch, M. J.; Sauter, G.; Kallioniemi, O. P., Tissue microarrays for high-throughput molecular profiling of tumor specimens. *Nat Med* **1998,** *4* (7), 844-7.
67. Ziauddin, J.; Sabatini, D. M., Microarrays of cells expressing defined cDNAs. *Nature* **2001,** *411* (6833), 107-10.

68. Xu, Q.; Lam, K. S., Protein and Chemical Microarrays-Powerful Tools for Proteomics. *J Biomed Biotechnol* **2003,** *2003* (5), 257-266.
69. Foong, Y. M.; Fu, J.; Yao, S. Q.; Uttamchandani, M., Current advances in peptide and small molecule microarray technologies. *Curr. Opin. Chem. Biol.* **2012,** *16* (1-2), 234-42.
70. Ma, H.; Horiuchi, K. Y., Chemical microarray: a new tool for drug screening and discovery. *Drug Discov Today* **2006,** *11* (13-14), 661-8.
71. (a) Lam, K. S.; Renil, M., From combinatorial chemistry to chemical microarray. *Curr. Opin. Chem. Biol.* **2002,** *6* (3), 353-8; (b) Uttamchandani, M.; Walsh, D. P.; Yao, S. Q.; Chang, Y. T., Small molecule microarrays: recent advances and applications. *Curr. Opin. Chem. Biol.* **2005,** *9* (1), 4-13; (c) Stockwell, B. R., Exploring biology with small organic molecules. *Nature* **2004,** *432* (7019), 846-54; (d) Walsh, D. P.; Chang, Y. T., Recent advances in small molecule microarrays: applications and technology. *Comb Chem High Throughput Screen* **2004,** *7* (6), 557-64; (e) He, X. G.; Gerona-Navarro, G.; Jaffrey, S. R., Ligand discovery using small molecule microarrays. *J. Pharmacol. Exp. Ther.* **2005,** *313* (1), 1-7.
72. Park, S.; Lee, M. R.; Pyo, S. J.; Shin, I., Carbohydrate chips for studying high-throughput carbohydrate-protein interactions. *J. Am. Chem. Soc.* **2004,** *126* (15), 4812-9.
73. Houseman, B. T.; Mrksich, M., Carbohydrate arrays for the evaluation of protein binding and enzymatic modification. *Chem. Biol.* **2002,** *9* (4), 443-54.
74. Kohn, M.; Wacker, R.; Peters, C.; Schroder, H.; Soulere, L.; Breinbauer, R.; Niemeyer, C. M.; Waldmann, H., Staudinger ligation: a new immobilization strategy for the preparation of small-molecule arrays. *Angew. Chem. Int. Ed. Engl.* **2003,** *42* (47), 5830-4.
75. Bryan, M. C.; Fazio, F.; Lee, H. K.; Huang, C. Y.; Chang, A.; Best, M. D.; Calarese, D. A.; Blixt, O.; Paulson, J. C.; Burton, D.; Wilson, I. A.; Wong, C. H., Covalent display of oligosaccharide arrays in microtiter plates. *J. Am. Chem. Soc.* **2004,** *126* (28), 8640-1.
76. de Paz, J. L.; Spillmann, D.; Seeberger, P. H., Microarrays of heparin oligosaccharides obtained by nitrous acid depolymerization of isolated heparin. *Chem Commun (Camb)* **2006,** (29), 3116-8.
77. Tully, S. E.; Rawat, M.; Hsieh-Wilson, L. C., Discovery of a TNF-alpha antagonist using chondroitin sulfate microarrays. *J. Am. Chem. Soc.* **2006,** *128* (24), 7740-1.
78. Blixt, O.; Head, S.; Mondala, T.; Scanlan, C.; Huflejt, M. E.; Alvarez, R.; Bryan, M. C.; Fazio, F.; Calarese, D.; Stevens, J.; Razi, N.; Stevens, D. J.; Skehel, J. J.; van Die, I.; Burton, D. R.; Wilson, I. A.; Cummings, R.; Bovin, N.; Wong, C. H.; Paulson, J. C., Printed covalent glycan array for ligand profiling of diverse glycan binding proteins. *Proc. Natl. Acad. Sci. U. S. A.* **2004,** *101* (49), 17033-8.
79. de Paz, J. L.; Noti, C.; Seeberger, P. H., Microarrays of synthetic heparin oligosaccharides. *J. Am. Chem. Soc.* **2006,** *128* (9), 2766-7.
80. (a) Fei, Y.; Landry, J. P.; Sun, Y.; Zhu, X.; Wang, X.; Luo, J.; Wu, C. Y.; Lam, K. S., Screening small-molecule compound microarrays for protein ligands without fluorescence labeling with a high-throughput scanning microscope. *J Biomed Opt* **2010,**

15 (1), 016018; (b) Landry, J. P.; Fei, Y.; Zhu, X. D., High Throughput, Label-free Screening Small Molecule Compound Libraries for Protein-Ligands using Combination of Small Molecule Microarrays and a Special Ellipsometry-based Optical Scanner. *Int Drug Discov* **2011**, 8-13.
81. Villiers, M. B.; Cortes, S.; Brakha, C.; Marche, P.; Roget, A.; Livache, T., Polypyrrole-peptide microarray for biomolecular interaction analysis by SPR imaging. *Methods Mol Biol* **2009,** *570*, 317-28.
82. Gurard-Levin, Z. A.; Scholle, M. D.; Eisenberg, A. H.; Mrksich, M., High-throughput screening of small molecule libraries using SAMDI mass spectrometry. *ACS Comb Sci* **2011,** *13* (4), 347-50.
83. Hsiao, H. Y.; Chen, M. L.; Wu, H. T.; Huang, L. D.; Chien, W. T.; Yu, C. C.; Jan, F. D.; Sahabuddin, S.; Chang, T. C.; Lin, C. C., Fabrication of carbohydrate microarrays through boronate formation. *Chem Commun (Camb)* **2011,** *47* (4), 1187-9.
84. Edwards, N. Y.; Sager, T. W.; McDevitt, J. T.; Anslyn, E. V., Boronic acid based peptidic receptors for pattern-based saccharide sensing in neutral aqueous media, an application in real-life samples. *J. Am. Chem. Soc.* **2007,** *129* (44), 13575-83.
85. Hsu, K. L.; Gildersleeve, J. C.; Mahal, L. K., A simple strategy for the creation of a recombinant lectin microarray. *Mol. BioSyst.* **2008,** *4* (6), 654-62.
86. Pilobello, K. T.; Krishnamoorthy, L.; Slawek, D.; Mahal, L. K., Development of a lectin microarray for the rapid analysis of protein glycopatterns. *ChemBioChem* **2005,** *6* (6), 985-9.
87. Hanzal-Bayer, M. F.; Hancock, J. F., Lipid rafts and membrane traffic. *FEBS Lett.* **2007,** *581* (11), 2098-104.
88. Forster, T., Delocalized excitation and excitation transfer. *Modern Quantum Chemistry* **1965,** *3.0*, 93-137.
89. Truong, K.; Sawano, A.; Mizuno, H.; Hama, H.; Tong, K. I.; Mal, T. K.; Miyawaki, A.; Ikura, M., FRET-based in vivo Ca2+ imaging by a new calmodulin-GFP fusion molecule. *Nat Struct Biol* **2001,** *8* (12), 1069-73.
90. Sekar, R. B.; Periasamy, A., Fluorescence resonance energy transfer (FRET) microscopy imaging of live cell protein localizations. *J. Cell Biol.* **2003,** *160* (5), 629-33.
91. Silvius, J. R.; Nabi, I. R., Fluorescence-quenching and resonance energy transfer studies of lipid microdomains in model and biological membranes. *Mol. Membr. Biol.* **2006,** *23* (1), 5-16.
92. Forster, T., Zwischenmolekulare Energiewanderung und Fluoreszenz. *Annalen der Physik* **1948,** *437*, 55–75.
93. Clegg, R. M., Fluorescence resonance energy transfer. *Curr. Opin. Biotechnol.* **1995,** *6* (1), 103-10.
94. Lakowicz, J. R., Principles of frequency-domain fluorescence spectroscopy and applications to cell membranes. *Subcell Biochem* **1988,** *13*, 89-126.
95. Wiskur, S. L.; Lavigne, J. J.; Metzger, A.; Tobey, S. L.; Lynch, V.; Anslyn, E. V., Thermodynamic analysis of receptors based on guanidinium/boronic acid groups for the complexation of carboxylates, alpha-hydroxycarboxylates, and diols: driving force for binding and cooperativity. *Chemistry* **2004,** *10* (15), 3792-804.

96. Springsteen, G., Wang B., A detailed examination of boronic acid-diol complexation. *Tetrahedron* **2002,** *58*, 5291-5300.
97. Gendler, S. J., MUC1, the renaissance molecule. *J Mammary Gland Biol Neoplasia* **2001,** *6* (3), 339-53.
98. (a) Kneeland, D. M.; Ariga, K.; Lynch, V. M.; Huang, C. Y.; Anslyn, E. V., BIS(ALKYLGUANIDINIUM) RECEPTORS FOR PHOSPHODIESTERS - EFFECT OF COUNTERIONS, SOLVENT MIXTURES, AND CAVITY FLEXIBILITY ON COMPLEXATION. *J. Am. Chem. Soc.* **1993,** *115* (22), 10042-10055; (b) Guy, J.; Caron, K.; Dufresne, S.; Michnick, S. W.; Skene, W. G.; Keillor, J. W., Convergent preparation and photophysical characterization of dimaleimide dansyl fluorogens: Elucidation of the maleimide fluorescence quenching mechanism. *J. Am. Chem. Soc.* **2007,** *129* (39), 11969-11977.

Appendix:

NMR Spectra

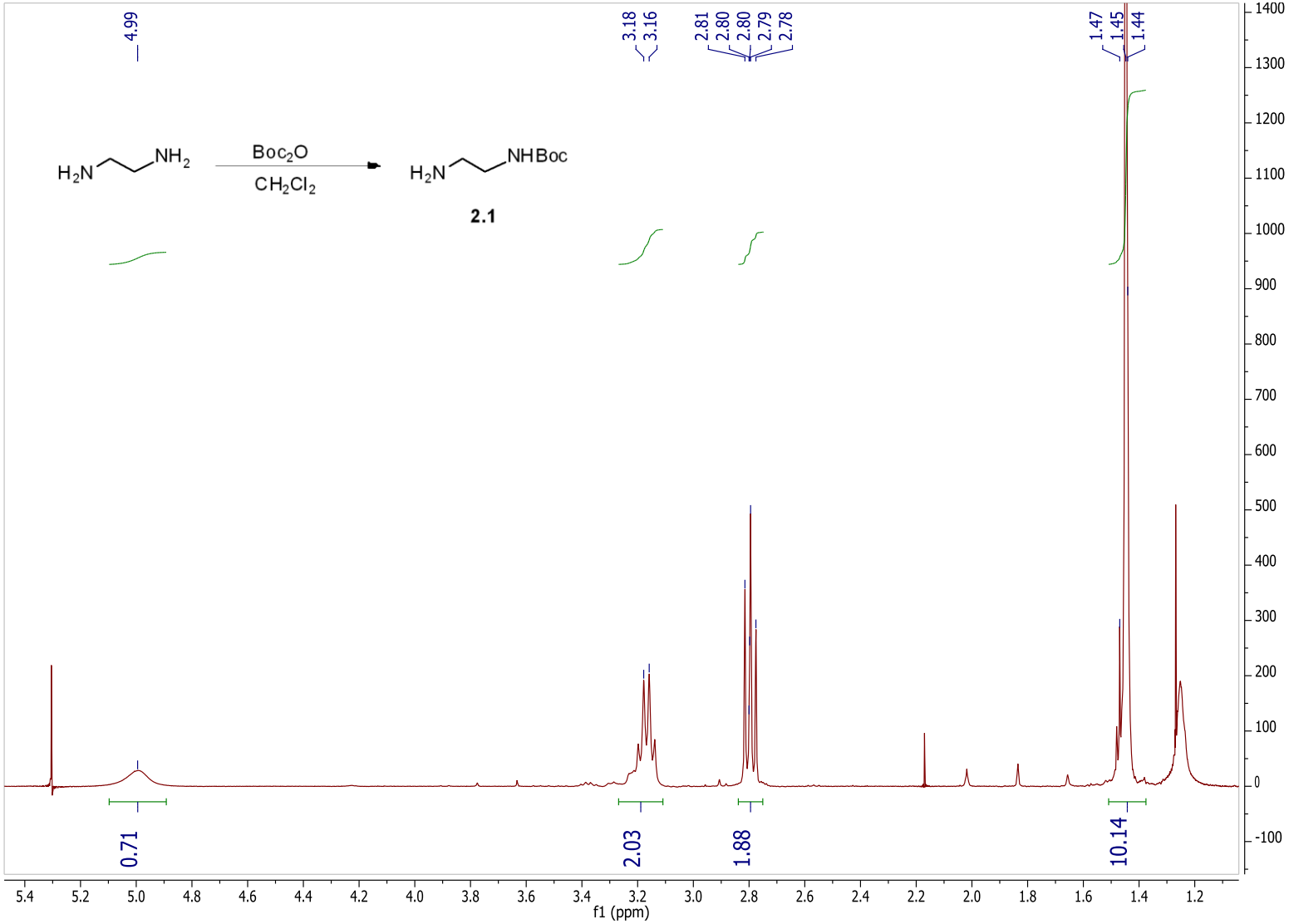
4.99
3.18
3.16
2.81
2.80
2.80
2.79
2.78
1.47
1.45
1.44
H2N
NH2
Boc2O
CH2Cl2
H2N
NHBoc
2.1
0.71
2.03
1.88
10.14
f1 (ppm)

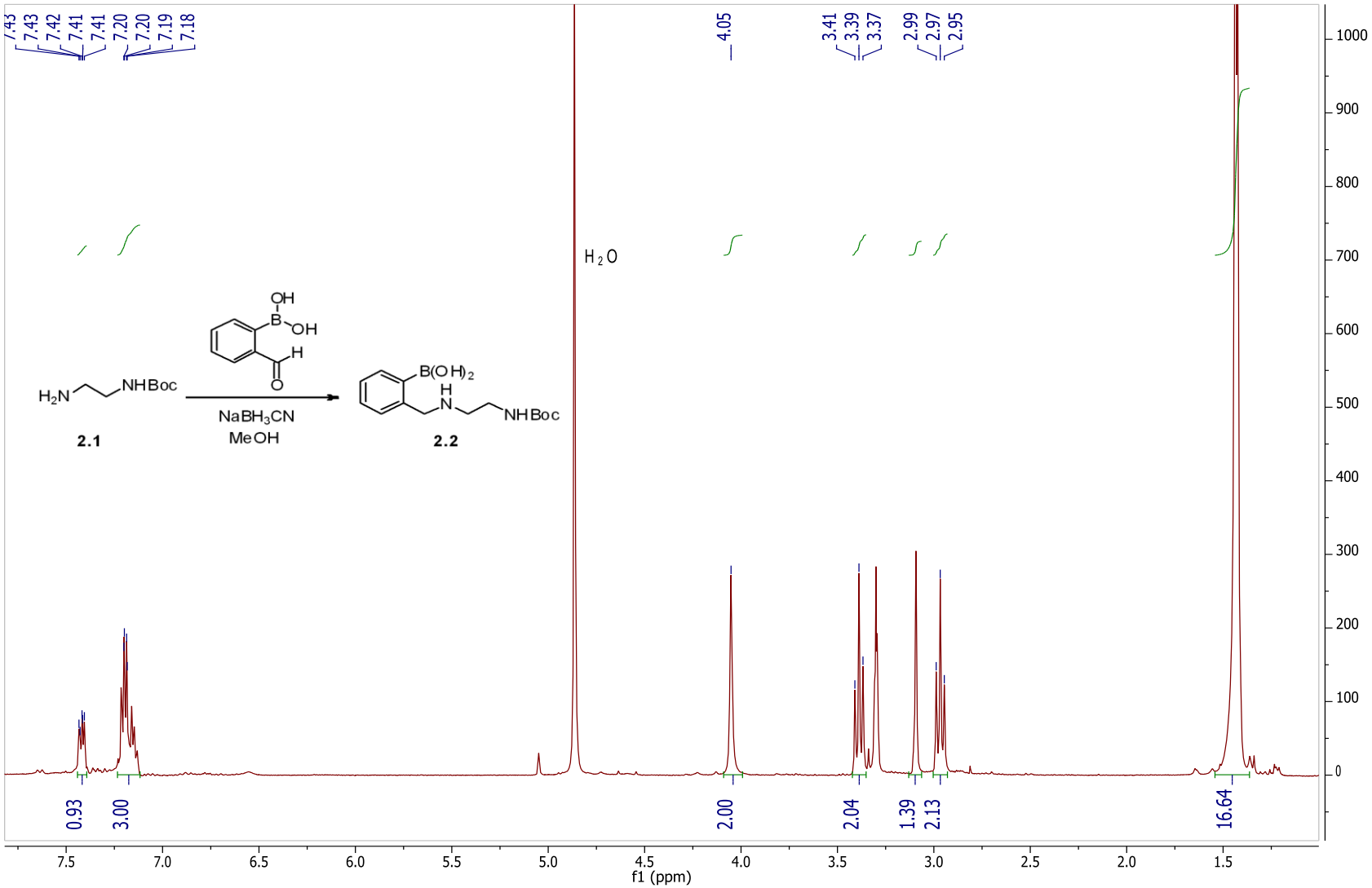
7.43
7.42
7.41
7.41
7.20
7.20
7.19
7.18
4.05
3.41
3.39
3.37
2.99
2.97
2.95
H2O
OH
B
OH
H
O
H2N
NHBoc
NaBH3CN
MeOH
2.1
B(OH)2
H
N
NHBoc
2.2
0.93
3.00
2.00
2.04
1.39
2.13
16.64
f1 (ppm)

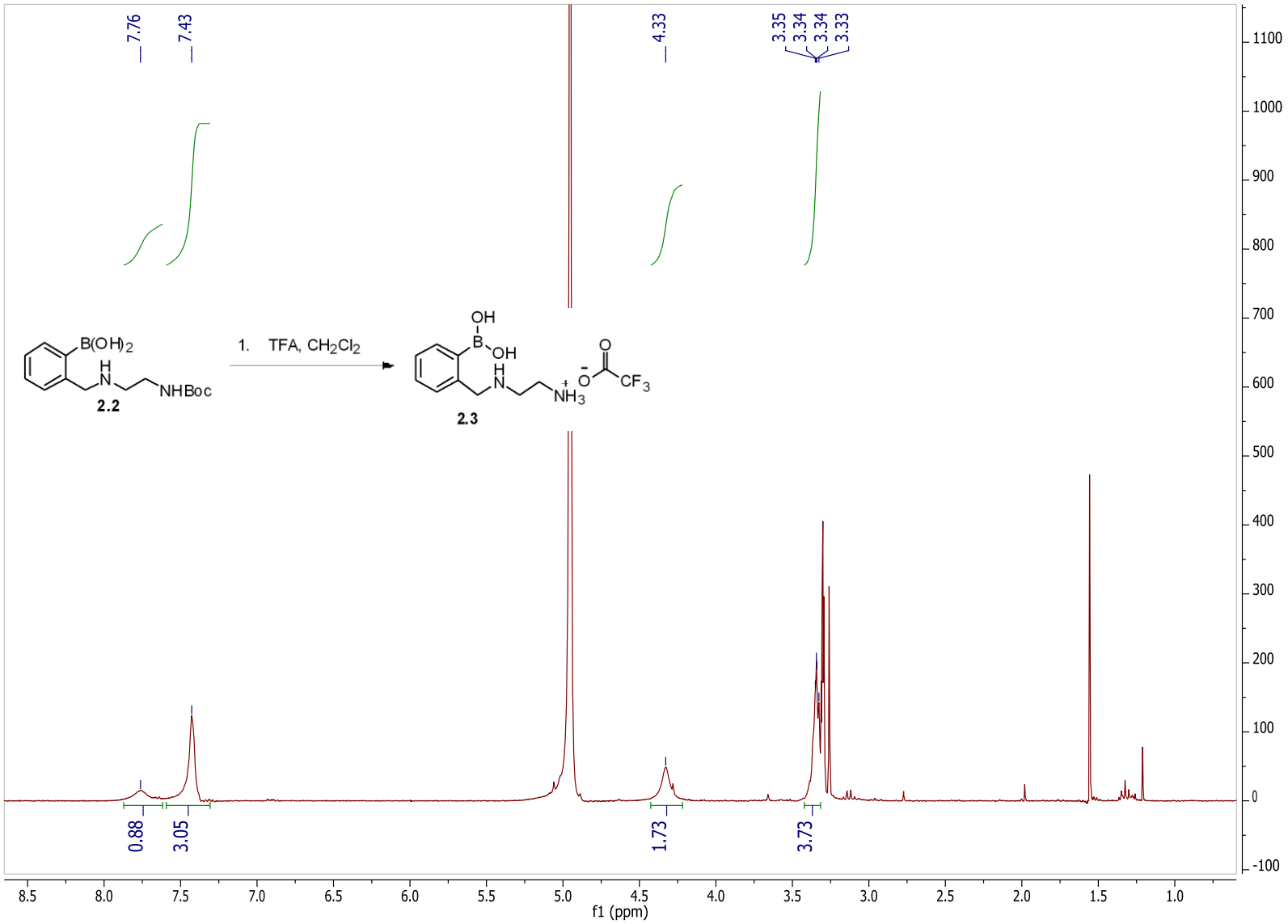
7.76
7.43
4.33
3.35
3.34
3.34
3.33
B(OH)2
H
N
NHBoc
2.2
1. TFA, CH2Cl2
OH
B
OH
H
N
O
O
CF3
NH3
2.3
0.88
3.05
1.73
3.73
f1 (ppm)

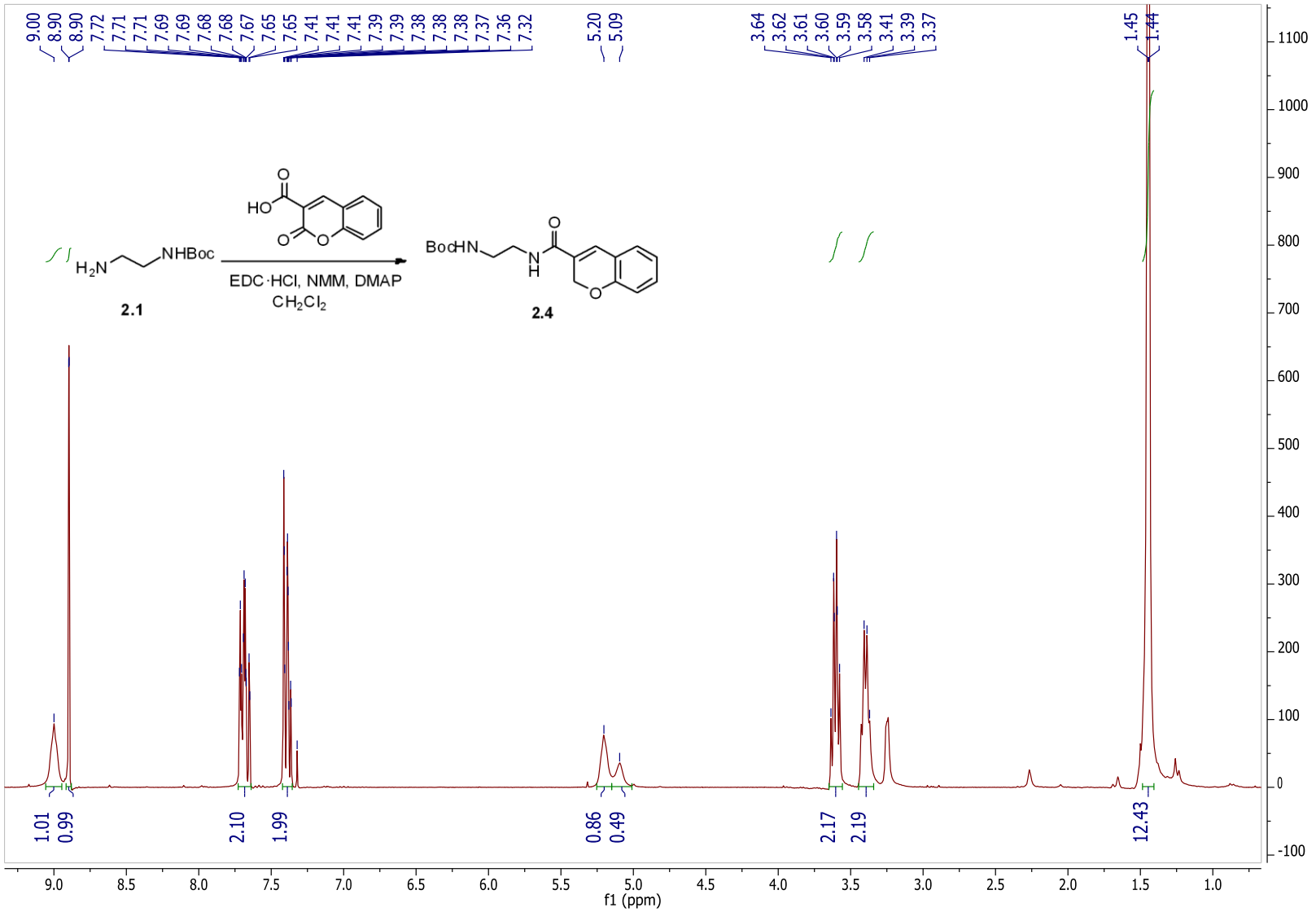
9.00
8.90
8.90
7.72
7.71
7.71
7.69
7.69
7.68
7.68
7.67
7.65
7.65
7.41
7.41
7.41
7.39
7.39
7.38
7.38
7.38
7.37
7.36
7.32
5.20
5.09
3.64
3.62
3.61
3.60
3.59
3.58
3.41
3.39
3.37
1.45
1.44
HO
O
O
O
H2N
NHBoc
2.1
EDC·HCl, NMM, DMAP
CH2Cl2
BocHN
N
H
O
O
2.4
1.01
0.99
2.10
1.99
0.86
0.49
2.17
2.19
12.43
f1 (ppm)

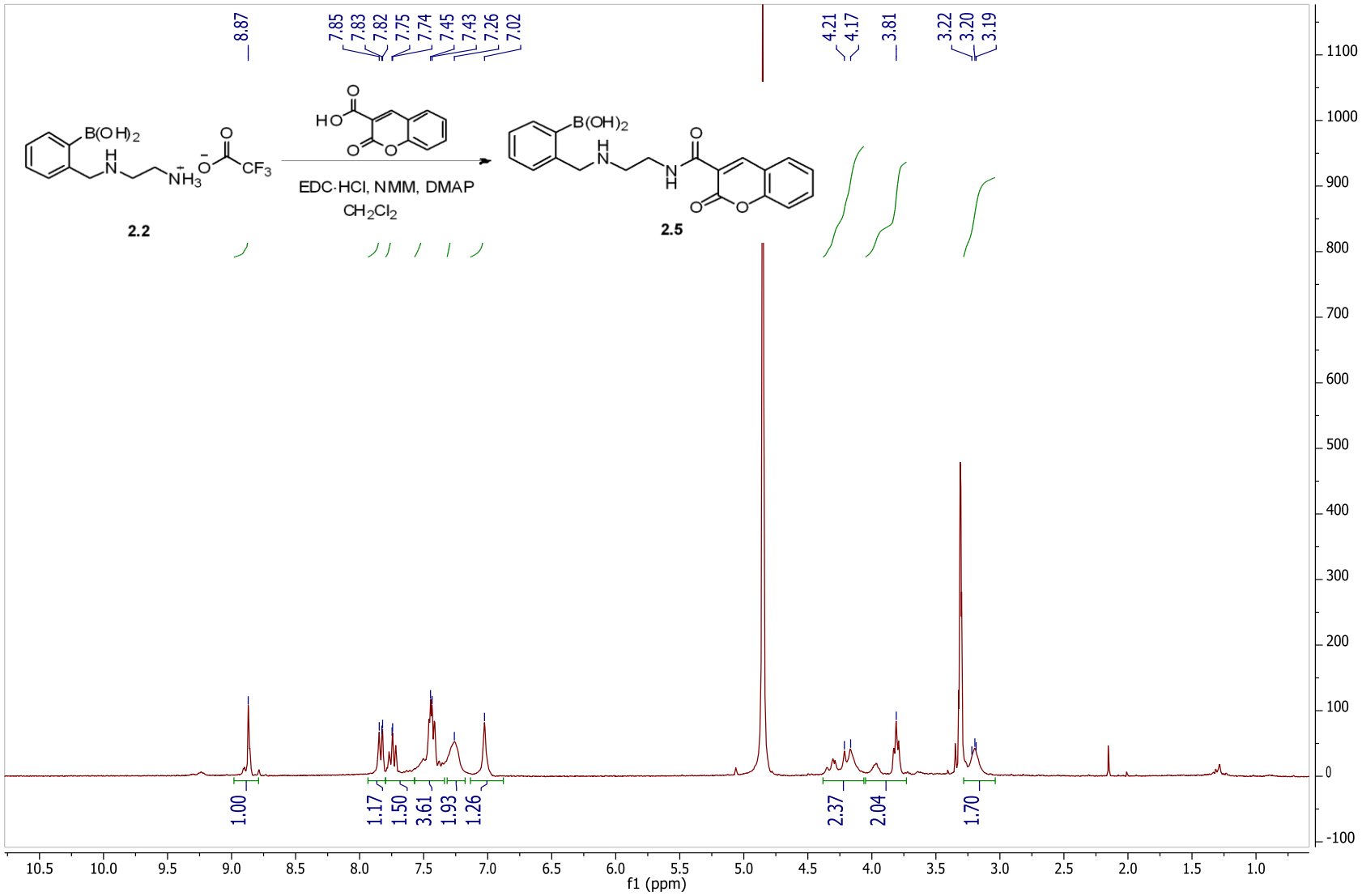
8.87
7.85
7.83
7.82
7.75
7.74
7.45
7.43
7.26
7.02
4.21
4.17
3.81
3.22
3.20
3.19
B(OH)2
NH3
CF3
2.2
EDC·HCl, NMM, DMAP
CH2Cl2
2.5
1.00
1.17
1.50
3.61
1.93
1.26
2.37
2.04
1.70
f1 (ppm)

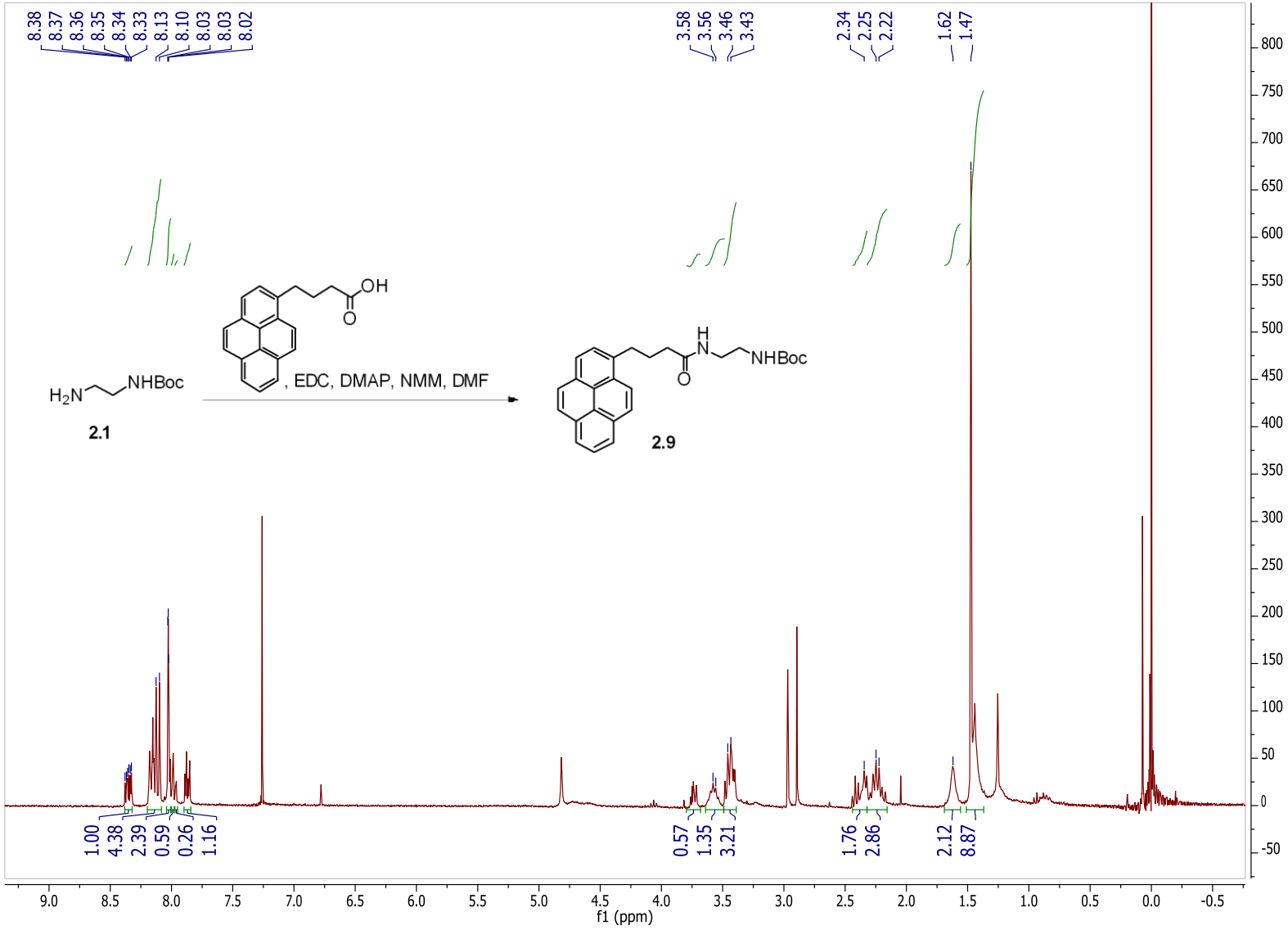
8.38
8.37
8.36
8.35
8.34
8.33
8.13
8.10
8.03
8.03
8.02
3.58
3.56
3.46
3.43
2.34
2.25
2.22
1.62
1.47
OH
O
, EDC, DMAP, NMM, DMF
H2N
NHBoc
2.1
H
N
O
NHBoc
2.9
1.00
4.38
2.39
0.59
0.26
1.16
0.57
1.35
3.21
1.76
2.86
2.12
8.87
f1 (ppm)

Vita

Yilin Wang was born in Shanghai, China in 1988. She moved with her parents to Singapore when she was six. After living in Singapore for ten years, she moved to Gainesville, Florida and completed her undergraduate education at the University of Florida. Despite being a proud gator, she went against her instincts and decided to pursue her graduate career at the University of Tennessee at Knoxville. Under the guidance of Dr. Michael Best, Yilin completed her Master's degree in Organic Chemistry in August 2012.